EC
Journals.ASM.org

Transcriptome and Functional Analysis of Mating in the Basidiomycete *Schizophyllum commune*

Susann Erdmann,[a] Daniela Freihorst,[a] Marjatta Raudaskoski,[b] Wolfgang Schmidt-Heck,[c] Elke-Martina Jung,[a] Dominik Senftleben,[a] and Erika Kothe[a]

Institute of Microbiology—Microbial Phytopathology, Friedrich-Schiller University, Jena, Germany[a]; Department of Biochemistry and Food Chemistry, Plant Physiology and Molecular Biology, University of Turku, Turku, Finland[b]; and Department of Molecular and Applied Microbiology, Leibniz Institute for Natural Product Research and Infection Biology—Hans Knöll Institute, Jena, Germany[c]

In this study, we undertook a functional characterization and transcriptome analysis that enabled a comprehensive study of the mating type loci of the mushroom *Schizophyllum commune*. Induced expression of both the *bar2* receptor and the *bap2(2)* pheromone gene within 6 to 12 h after mates' contact was demonstrated by quantitative real-time PCR. Similar temporal expression patterns were confirmed for the allelic *bbr1* receptor and *bbp1* pheromone-encoding genes by Northern hybridization. Interestingly, the fusion of clamp connections to the subterminal cell was delayed in mating interactions in which one of the compatible partners expressed the *bar2* receptor with a truncated C terminus. This developmental delay allowed the visualization of a green fluorescent protein (Gfp)-labeled truncated receptor at the cell periphery, consistent with a localization in the plasma membrane of unfused pseudoclamps. This finding does not support hypotheses envisioning a receptor localization to the nuclear membrane facilitating recognition between the two different nuclei present in each dikaryotic cell. Rather, Gfp fluorescence observed in such pseudoclamps indicated a role of receptor-pheromone interaction in clamp fusion. Transcriptome changes associated with mating interactions were analyzed in order to identify a role for pheromone-receptor interactions. We detected a total of 89 genes that were transcriptionally regulated in a mating type locus *A*-dependent manner, employing a cutoff of 5-fold changes in transcript abundance. Upregulation in cell cycle-related genes and downregulation of genes involved in metabolism were seen with this set of experiments. In contrast, mating type locus *B*-dependent transcriptome changes were observed in 208 genes, with a specific impact on genes related to cell wall and membrane metabolism, stress response, and the redox status of the cell.

The filamentous fungus *Schizophyllum commune* is a widely distributed mushroom that lives saprophytically and can cause white rot on wood. It has been extensively used to study mating interactions for almost 100 years (47). In addition to studies involving the mushroom *Coprinopsis cinerea* and the corn smut *Ustilago maydis*, the mating type genes have been extensively analyzed for this tetrapolar basidiomycete (4, 29). The recent publication of the *S. commune* genome sequence enables global expression analyses (41). During the life cycle of this fungus, compatible haploid monokaryons can mate to produce a fertile dikaryon with two nuclei per cell, one derived from each mating partner. Under appropriate environmental conditions, the dikaryon is able to form the sexual reproductive fruiting bodies (40). While the fusion of two monokaryotic hyphae (plasmogamy) is independent of mating types, specific steps of sexual development are regulated by the mating type genes encoded in the loci *A* and *B* (25, 47). For each of these loci, two linked, multiallelic subloci (termed α and β) have been determined by recombination analyses (27, 49, 51, 65). The *A* loci encode homeodomain transcription factors, while the *B* loci code for multiallelic pheromone receptors and pheromones (55, 63, 66). Both the *A* and *B* pathways can be activated by the combination of different allelic specificities in at least one subblocus derived from each of the two mates (46, 52, 53). Thus, for a compatible mating interaction to occur, different *A* and *B* mating types ($A{\neq}B{\neq}$) in the partners are essential.

The migration of nuclei is triggered by the presence of different *B* mating types after the fusion of two compatible monokaryons and occurs reciprocally from one mating partner throughout the mycelium of the other (54). Subsequent nuclear pairing, as well as the initiation of clamp cell development, is regulated by the *A* mating type. The formation of clamp cells at the septa of the developing dikaryon results in a regular distribution of the two different nuclei during mitosis within the dikaryon (4, 39). The last step of clamp fusion is dependent on different *B* factors and involves Ras signaling (31, 59). This sequence of events can be observed in semicompatible mating interactions where a heterokaryon with an activated *B* locus (B_{on} or $A{=}B{\neq}$) undergoes constant nuclear migration associated with irregular distribution of nuclei (26, 38). This phenotype, termed flat, results in reduced aerial mycelia, malformed hyphae, and no formation of clamps (43, 48). The second type of semicompatible mating interaction occurs with an activated *A* locus (A_{on} or $A{\neq}B{=}$) and is evident in the formation of pseudoclamps and a die-off in the contact zone (barrage phenotype) (38, 43, 44).

For the pheromone-receptor system encoded in the *B* locus of *S. commune*, the pheromone signaling is triggered by the interaction of nonself-pheromones with G-protein-coupled receptors (GPCRs) of class D (1, 20, 70). All pheromone receptors of basidiomycetes belong to the *Saccharomyces cerevisiae* Ste3-related pheromone receptor family and bind **a**-factor-related lipopeptide pheromones (12, 32, 67, 64). Multiple different cognate phero-

Received 22 August 2011 **Accepted** 22 December 2011
Published ahead of print 30 December 2011
Address correspondence to Erika Kothe, erika.kothe@uni-jena.de.
Supplemental material for this article may be found at http://ec.asm.org/.

doi:10.1128/EC.05214-11

TABLE 1 *Schizophyllum commune* strains and mating interactions

Strains and crosses	Mating type, relevant genotype/description
H4-8	$A_{4,6}$;$B_{3,2}$
W21	$A_{1,1}$;$B_{1,1}$
W22	$A_{4,6}$;$B_{3,2}$
W22-thin	$A_{4,6}$;$B_{3,2}$; thin (thin[a])
V153-21	$A_{3,5}$;B_{null}; *trp1*$^-$
Vbar2f	$A_{3,5}$;B_{null}::*bar2 trp1*
Vbar2t	$A_{3,5}$; B_{null}::*bar2*ΔPstI *trp1*
Vbar2tG1	$A_{3,5}$;B_{null}::*bar2*ΔPstI-HA-Gfp *trp1*
Vbar2tG11	$A_{3,5}$;B_{null}::*bar2*ΔPstI-HA-Gfp *trp1*
12-43	$A_{3,5}$;$B_{2,3}$; *ura1*$^-$; monokaryon (Mon1[a])
4-39	$A_{1,1}$;$B_{3,2}$; monokaryon (Mon2[a])
W22 × 12-43	Dikaryon (Dik[a])
W22 × 4-39	Semicompatible interaction: $A\neq B=$ (A_{on}[a])
W21 × 4-39	Semicompatible interaction: $A=B\neq$ (B_{on}[a])
Vbar2f × 4-39	Dikaryon of receptor transformant with full-length receptor (Dik-Vbar2f[a])
Vbar2t × 4-39	Dikaryon of receptor transformant with truncated receptor (Dik-Vbar2t[a])

[a] Term for microarray analysis.

mones capable of activating a single receptor in a multistate model of interaction have evolved in *S. commune*, most likely by recombination between copies of the mating type locus (15, 20). The function of pheromone signaling is thus linked to the processes of nuclear migration, nuclear identity, and clamp fusion.

A model that links pheromone-receptor interactions to the distance between nuclei in dikaryons had been proposed. Under this model, productive interaction between non-self-pheromones and their cognate receptor occurs only when the nuclei are in close proximity to each other (60). Another hypothesis (5) proposed that receptor localization to the nuclear envelope was necessary for detection of intracellular pheromone(s). This would necessitate an inverse orientation of the receptor within the membrane. In order to investigate the role of the pheromone receptor and to distinguish between the different models described above, receptor localization has been of great interest for a number of years. A plasma membrane localization was found for pheromone receptors in single cells of the corn pathogen *U. maydis* (17). In mushroom-forming homobasidiomycetes like *S. commune* or *C. cinerea*, however, cellular localization of the pheromone receptor has not yet been determined.

The role of pheromone perception in *S. cerevisiae* includes both mate attraction and the formation of shmoo cells that show growth directed toward the mating partner (33). In contrast, attraction and fusion of *S. commune* hyphae can be seen independent of mating type. Directional growth toward a mate has been observed at very short distances (54). In an earlier investigation on the role of Ras in sexual development of *S. commune*, we demonstrated that a deletion of a Ras-specific GTPase-activating protein, Δ*gap1*, results in a lack of clamp fusion in Δ*gap1* homoallelic dikaryons (59). This uninucleate state is rescued by development of a branch, which is then able to fuse with the clamp cell after prolonged growth. We hypothesized that this situation in the mutant represents two monokaryotic cells which show clear attraction toward each other. Thus, clamp fusion in dikaryons can be viewed as a system in which mate attraction can be visualized at very short distances.

The intracellular signaling via GPCRs has been shown to be controlled by regulators of G-protein signaling (RGS) in other studies of *S. commune* (6, 13). The RGS protein Thn1 negatively regulates the activity of the G-protein α subunit by acting as a GTPase-activating protein (GAP) (42). A loss-of-function mutation due to transposon integration into *thn1* results in hyphae with a characteristic corkscrew morphology which are unable to accept nuclei of a compatible mating partner (13, 61). For *S. cerevisiae*, RGS gene *SST2* was functionally linked to mating interactions (7, 8).

In the study presented here, we show the localization of the G-protein-coupled pheromone receptor protein in hyphal filaments of *S. commune*. Furthermore, we report on the role of the C-terminal region of the pheromone receptor Bar2 in mating interactions. In combination with transcriptome analyses, a comprehensive study of the pheromone-receptor system for a mushroom-forming basidiomycete is presented for the first time.

MATERIALS AND METHODS

Strains and culture conditions. The *S. commune* strains 4-40, 23, 684, 1792-114-10, W21, W22, W22-thin, V153-21 (B_{null}), 12-43, and 4-39 were obtained from the Jena Microbial Resource Center (JMRC) or the strain collection of University of Turku. *S. commune* receptor transformants generated in this study (Vbar2f, Vbar2t, Vbar2tG1, Vbar2tG11) and strains relevant for microarray analysis are listed in Table 1. *S. commune* was routinely grown at 28°C on minimal medium (MM) (50) or complex yeast medium (CYM) (62) with 2% (wt/vol) glucose, with or without 1.8% (wt/vol) agar. Liquid cultures were shaken at 150 rpm. For RNA extraction, cultures were grown on a cellophane membrane placed on solid medium. The *S. commune* strains investigated by Northern blotting or quantitative real-time PCR (RT-PCR) were cultured using a modified sandwich method as described previously (67). Interacting mycelia were grown for 3 to 72 h at 28°C before harvest. For transcriptome analysis, mycelia from a monokaryon or a mating interaction were transferred onto a cellophane membrane placed on fresh CYM plates and grown for 3 days.

Functional analysis and receptor localization. We generated the transformants that are expressing Vbar2f using a B_{null} strain, which untransformed does not expresses mating pheromones or receptors (14). For amplification of the pheromone receptor gene *bar2f* (NCBI accession number X91168.4), we used primers S1 (5′-GGATCCGCCCATTGTCC-3′) and S2 (5′-TCACACCGACGCGCGGT-3′) to produce an amplicon starting from approximately 300 bp upstream of ATG and extending to the last 17 bases of *bar2* (Fig. 1). Comparison of the last 17 bases of *bar2* with those in *bar1* and *bar3* shows that they are identical, except for a different stop codon in *bar3*. The pheromone receptor gene *bar2f* encodes a full-length protein of 636 amino acids (aa). In addition, we generated the strain Vbar2t, which was transformed with a mutated gene encoding a

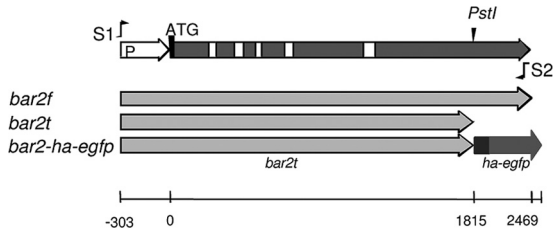

FIG 1 Gene *bar2* of *Schizophyllum commune*. The primers S1 and S2 were used for amplification of full-length gene *bar2f* (NCBI accession number X91168.4) with promoter region (P). The gene *bar2t* was truncated at the 3′ PstI restriction site (see also NCBI accession number X91168.2). The 3× HA-eGfp tag (*ha-egfp*) is indicated at the C terminus of the *bar2t* gene. The white squares indicate introns.

truncated receptor of *Bα2* specificity with 518 aa in length; the sequence of *bar2t* is truncated at a 3′ PstI site (20) (NCBI accession number X91168.2, GI 23954358). The truncated *bar2t* receptors of strains Vbar2tG1 and Vbar2tG11 have been tagged with extended green fluorescent protein (eGfp) for *in vivo* studies and with hemagglutinin (3× HA) for receptor localization by indirect immunostaining. The HA-eGfp sequence (845 bp) was amplified with the primers 5′-GGC TGC AGG GAT ACC CGT ATG ATG TTC CGG ATT ACG CTG GCT ACC CAT ACG ACG TCC CAG ACT ACG CTG GCT ACC CAT ACG ACG TCC CAG ACT ACG CTG GCG CAC CTG GAG CCA TGG TGA GCA AGG GCG AGG AGC-3′and 5′-GTT GGA ATT CTG CAG TCG CGG CCG CTT TAC TTG-3′ using the vector pegfp (Clontech, The Netherlands) as template and ligated into the PstI site at the C terminus of *bar2t*. All transformed pheromone receptor genes were expressed under their native promoter.

Fluorescence microscopy and immunostaining. For microscopic analysis, sterile glass coverslips were placed on an agar plate such that hyphae could attach to and grow onto the slides after 2 to 4 days of cultivation. Mycelia of *S. commune* were fixed for 90 min at room temperature with methanol and PME {50 mM PIPES [piperazine-*N*,*N*′-bis(2-ethanesulfonic acid)], pH 6.7, 25 mM EGTA, pH 8.0, 5 mM $MgSO_4$} plus 3.7% formaldehyde. Coverslips were then washed with PME and the cells were treated with 3% lysis enzyme (*Trichoderma harzianum*; L1412; Sigma, Germany) and 50% egg white. The cells were permeabilized with 0.3% Triton X-100 in phosphate-buffered saline (PBS; 137 mM NaCl, 2.68 mM KCl, 8.09 mM Na_2HPO_4, 1.76 mM KH_2PO_4, pH 7.4). Nonspecific binding sites were blocked with 3% bovine serum albumin (BSA). The 1st antibody (mouse anti-HA 2367; Cell Signaling) was diluted 1:200 in PBS with 3% BSA, and coverslips were incubated overnight at 4°C. The fluorescein isothiocyanate (FITC)-labeled 2nd antibody (FITC-antimouse; F4018; Sigma) was diluted 1:100 in PBS and incubated for 60 min at 37°C. Following every incubation step, the coverslips were washed with PBS at least once. Nuclei were stained with DAPI (4′,6-diamidino-2′-phenylindole dihydrochloride; 0.1 to 1 μg/ml) added to the mounting medium (0.1 M Tris HCl, pH 8.0, 50% glycerol, and 1 mg/ml phenylenediamine). The mycelia were examined with a fluorescence microscope (Axioplan2) and confocal laser scanning microscope (LSM 5 Live) (Carl Zeiss MicroImaging, Jena, Germany). Images were processed with SPOT imaging software (Diagnostic Instruments, Sterling Heights, MI) and ZEN software (Carl Zeiss, Jena, Germany).

Quantitative real-time PCR and Northern hybridization. Mycelia were harvested, frozen in liquid nitrogen, and ground with mortar and pestle to a powder. Total RNA was isolated from not more than 100 mg of tissue powder using a commercial kit (RNeasy plant minikit; Qiagen, Hilden, Germany). Reverse transcription was performed using 1 μg of total RNA in a 20-μl reaction mix (iScript cDNA synthesis kit; Bio-Rad, Munich, Germany). For each real-time PCR, we used 2 μl of cDNA as template in a 25-μl reaction mix that additionally contained 12.5 μl 2× reaction mix [1.25 U Hot *Taq* DNA polymerase, 0.4 mM deoxynucleoside triphosphates, 40 mM Tris HCl, pH 8.55, 32 mM $(NH_4)_2SO_4$, 0.02% Tween 20, and 4 mM $MgCl_2$; peqGold hot start mix Y; Peqlab], 7.5 μl water (nuclease free), 1 μl of each primer (10 pmol/μl), and 1 μl SYBR green I (using a 1:2,000 dilution of the stock reagent; Molecular Probes, Invitrogen) using a SmartCycler II thermocycler (Cepheid). The PCR program consisted of 5 steps (initial denaturation for 120 s at 94°C; 45 cycles of denaturation for 20 s at 94°C, annealing for 20 s at 50 or 55°C, and extension for 20 s at 72°C; and a final melting curve analysis at 60 to 95°C with 0.2°C/s). The SYBR green fluorescence was detected (excitation, 450 to 495 nm; emission, 510 to 527 nm) during both the extension phase of each cycle and the subsequent melting curve analysis. For amplification of the target genes *bar2* and *bap2(2)*, as well as the reference genes *act1* and *tef1*, the following oligomers were used: 5′-ATTACTCTTGGCGCCTCT GTA-3′ and 5′-AATGAGAGCGTCGACCATGACT-3′ for *bar2* (yielding a product of 138 bp), 5′-TTACTGATAGTCACAGATA-3′ and 5′-ATGG CGAACCGGAC-3′ for *bap2(2)* (87 bp), 5′-GTCCGCCCTCGAGAAGA GTTA-3′ and 5′-TTGTACGTCGTCTCGTGGATA-3′ for *act1* (141 bp), and 5′-AGCTTGGCAAGGGTTCCTTCA-3′ and 5′-AACTTCCAGAGG GCGATATCA-3′ for *tef1* (97 bp). The primers for *bar2*, *act1*, and *tef1* span an intron to identify potential genomic DNA contamination. The gene *bap2(2)* has a total length of only 87 bp and has no intron. Annealing was performed at 55°C for all genes except *bap2(2)*, which was amplified at an annealing temperature of 50°C. The calculation of the gene-specific efficiencies was based on the slope of a standard curve generated from a series of different cDNA concentrations (0.04, 0.2, 1, 5, 25, 50, 100, and 200 ng cDNA/25-μl PCR mixture). cDNA was derived from a mating interaction between two compatible wild-type strains (12-43 × 4-39). The PCR efficiency for *bar2* was 1.83 (corresponding to 83% of exponential expression), that for *bap2(2)* was 1.53 (53%), that for *act1* was 2.1 (110%), and that for *tef1* was 2.0 (100%).

Since the receptor and pheromone genes between different strains are not alike at the DNA sequence level but belong to the same family of gene products, the primer combinations were tested with templates of different *Bα* specificities. The receptor and pheromone primers gave no amplification with specificities other than *Bα2* (data not shown). The genes *act1*, coding for actin, and *tef1*, coding for translation elongation factor EF1α, were suitable reference genes with stable expression levels under the tested conditions.

The expression of the target genes was determined relative to the expression of reference genes, which were used for the normalization of expression between samples. We measured expression levels in mycelia isolated at a progression of different times during the mating interaction (after 3, 6, 9, 12, 24, 30, 48, 54, and 72 h; samples t_3 through t_{72}). These times correspond to mycelia of different nuclear distributions. Sample t_0 corresponds to a mix of two monokaryons which have been brought together directly before sampling (t_0 = monokaryon, 0 h) and reflects the basal level of expression (control). For each time and individual mating interaction, the total RNAs of three independently grown mycelia have been isolated and transcribed into cDNA in duplicate, and each one was used as a template in real-time PCR, also measured in duplicate. The expression of the target genes was normalized and quantified relative to the expression of the reference genes and was also corrected for the calculated efficiency (45, 68). Northern hybridization experiments and the labeling of the receptor and pheromone cDNA fragments were performed as described previously (21).

Microarray-based transcriptome analysis. Quantification of transcriptome changes associated with mating interactions was performed in order to identify signaling components and targets of pheromone response. In addition, an *S. commune* strain showing the thin phenotype was investigated to resolve the role of Thn1 in mating. The microarrays (febit biomed GmbH, Heidelberg, Germany) used in the present study contain probes for all 13,181 predicted genes of *S. commune*. It is based primarily upon the November 2008 version of the *Schizophyllum commune* (version 1.0) genome using strain H4-8 ($A_{4,6}$;$B_{3,2}$). The probes (oligonucleotides of ~50 bases in length) have been spotted on Geniom Biochips. The strains and mating interactions were investigated in microarray analysis in two biological or technical replicates (Table 1; see also Table S1 in the supplemental material). Genes which show regulation (fold change, ≥2) between the two monokaryotic strains 12-43 and 4-39 were eliminated from all other comparisons as strain-specific differences (Fig. 2).

A comparison of the A_{on} condition versus 4-39 (Mon2) yielded what were defined to be *A*-regulated genes. In contrast, *B*-regulated genes were defined by comparing B_{on} versus Dik: this assumes that hyphae activated for *B*-dependent regulation (B_{on}) are more related to dikaryotic hyphae containing nuclei of both mating partners after nuclear migration. At the same time, no gene was included from the former set (*A*-regulated genes) so as not to involve cross-pathway signaling between *A* and *B* (Fig. 2).

Differentially expressed genes of the thin phenotype were up- or downregulated in both of the comparisons made: 12-43 (Mon1) versus W22-thin and 4-39 (Mon2) versus W22-thin (Fig. 2). To identify regulated genes influenced by the C-terminal region of Bar2, we defined two criteria: genes had to be up- or downregulated in both comparisons: Dik-

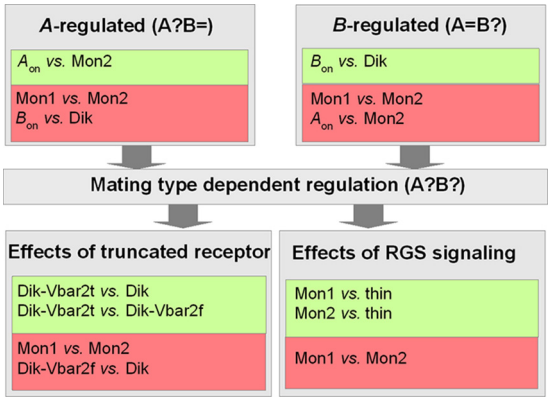

FIG 2 Diagram of interactions screened to identify genes differentially regulated. The comparison of assumed different (green) and similar (red) interactions was used to identify genes regulated in transcriptome profiling.

Vbar2t versus Dik and Dik-Vbar2t versus Dik-Vbar2f. In addition, these genes were unregulated in Dik-Vbar2f versus Dik (Fig. 2).

For each array, 1 μg of total RNA was labeled using the MessageAmp-biotin enhanced RNA kit from Ambion. Hybridization was performed automatically for 16 h at 45°C using RT-Analyzer (febit, Heidelberg, Germany). The biotin-labeled nucleic acid was detected using streptavidin-phycoerythrin (SAPE) in combination with consecutive signal enhancement (CSE). Feature recognition using the Cy3 filter set and signal calculation were automatically analyzed within milliseconds using the Geniom RT-Analyzer (febit, Heidelberg, Germany). For preprocessing, all data analyses of the febit microarrays were performed using the LIMMA (linear models for microarray data) packages of the Bioconductor software (18). Background correction was performed using the intensities of blank probes that consisted of only a single T nucleotide. The median background intensity was subtracted from the spot intensity. After converting any negative values to a low-positive value (8), signal intensities were $\log_2$ transformed, and duplicate spots were averaged. The data obtained were processed using quantile normalization. To identify the genes with the greatest evidence of differential expression, a linear model fit was applied for each gene using LIMMA. Candidate genes were selected for further analysis on the basis of their fold change (≥5) in expression and their *P* value (≤0.05).

Microarray data accession number. The data discussed in this publication have been deposited in NCBI's Gene Expression Omnibus (9) and are accessible through GEO Series accession number GSE26401 (http://www.ncbi.nlm.nih.gov/geo/query/acc.cgi?acc=GSE26401).

RESULTS

Expression of pheromone receptor and pheromone genes during mating interactions. In order to assess the expression of both pheromone receptor and pheromone genes during the life cycle of *S. commune*, a specific pheromone receptor gene, *bar2*, and a corresponding self-pheromone gene, *bap2(2)*, were analyzed by quantitative real-time PCR. As expected, expression levels for both mating type-specific genes were low in monokaryons (t_0), and expression was specifically induced during mating interactions. In a time series from 0 to 72 h (t_0 to t_{72}) during a compatible mating interaction, the expression of the receptor gene *bar2* increased gradually to a 3-fold higher level in the first 9 h and reached a maximal change of 8-fold after 12 h (Fig. 3). Subsequently, the expression of *bar2* gradually decreased to a low level comparable to monokaryotic expression levels. The expression of the pheromone gene *bap2(2)* increased to a maximum of a 3-fold increase over baseline after 12 h, decreasing shortly thereafter (Fig. 3). In contrast to the receptor, however, pheromone expression increased steadily and then again up to 2.5-fold after 72 h. Overall, the expression levels of receptor gene *bar2* and pheromone gene *bap2(2)* in wild type were extremely low, reaching the threshold level only after 26 and 29 to 32 cycles, respectively, while the reference genes *act1* and *tef1* amplified with mean threshold cycles of 15 and 21, respectively.

The quantitative RT-PCR measurements of *bar2* and *bap2(2)* were in accordance with those from Northern blot experiments determining both *bbr1* receptor and *bbp1(1)* pheromone gene expression in a time series from 3 to 12 h (Fig. 4). Induction of genes encoding receptors *bar1* and *bbr1* as well as pheromones *bbp1(1)*, *bbp1(2)*, and *bbp1(3)* was obtained in A_{on} and B_{on} semicompatible matings, although the signals in these

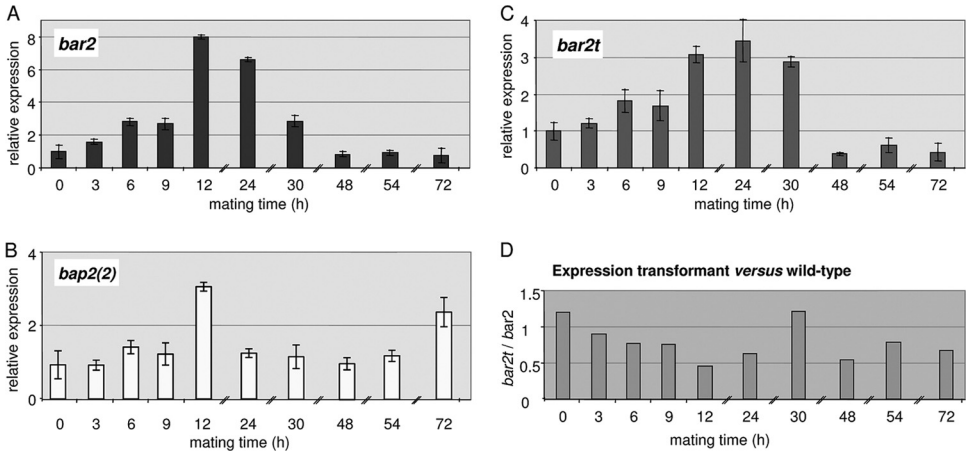

FIG 3 (A and B) Expression of the pheromone receptor gene *bar2* (A) and the pheromone gene *bap2(2)* (B) in a wild-type mating (12-43 × 4-39); (C) expression of a truncated version of pheromone receptor gene *bar2t* in the transformant Vbar2t in a mating with the wild-type strain 4-39. The gene expression levels were determined by quantitative real-time PCR of compatible mating interactions over a time period of 72 h. The expression levels in monokaryons (t_0) were normalized to 1, and all other mating times (t_3 to t_{72}) are shown relative to t_0. (D) Ratio of *bar2t*/*bar2* expression, illustrating the effect of a C-terminal truncation of the pheromone receptor.

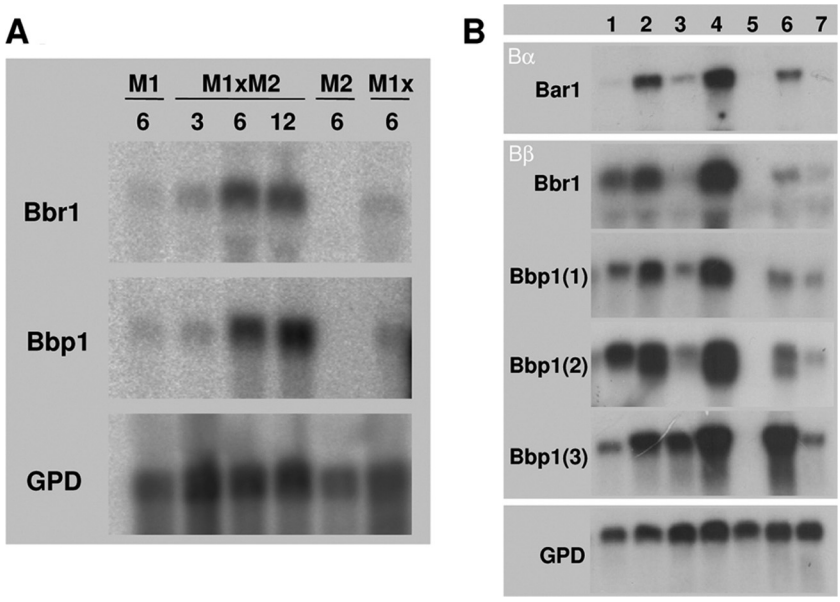

FIG 4 Northern hybridization of receptor and pheromone gene expression during compatible and semicompatible matings. (A) Expression of the Bbr1 receptor and the Bbp1 pheromone-encoding genes in a compatible mating, 4-40 (M1; $A_{4,6};B_{1,1}$) × 4-39 (M2; $A_{1,1};B_{3,2}$), and the two respective monokaryons, as well as an incompatible cross between identical monokaryons (M1x). RNA extraction was performed after the indicated times (3, 6, 12 h). (B) Expression of the receptor genes encoding Bar1 and BbrI and also those encoding the pheromones Bbp1(1), Bbp1(2), and Bbp1(3). Lane 1, expression in A_{on} semicompatible mating between strains 23 ($A_{4,6};B_{3,1}$) × 684 ($A_{2,6};B_{3,1}$); no signal was expected for *bar1* since neither of the *B* loci encodes the *bar1* receptor; lanes 2 and 3, B_{on} semicompatible matings between strains 1792-114-10 ($A_{4,6};B_{3,6}$) × 4-40 ($A_{4,6};B_{1,1}$) and 43/26 ($A_{4,6};B_{3,1}$) × 4-40 ($A_{4,6};B_{1,1}$), respectively; lane 4, $A_{on};B_{on}$ fully compatible mating between strains 4-40 ($A_{4,6};B_{1,1}$) × 4-39 ($A_{1,1};B_{3,2}$); lane 5, strain 4-39 ($A_{1,1};B_{3,2}$); no signal was expected in this control since no sequences encoding either the Bar1 and Bbr1 receptor or any of the three Bbp1 pheromones are present in strain 4-39; lane 6, strain 4-40 ($A_{4,6};B_{1,1}$); lane 7, strain 23 ($A_{4,6};B_{3,1}$). All strains were grown for 8 h after mating. Each well contains 20 μg of total RNA. Expression of glyceraldehyde-3-phosphate dehydrogenase (GPD) was monitored as a loading control.

interactions were lower than those in a compatible mating leading to dikaryon formation (Fig. 4).

The pheromone receptors of *S. commune* contain long intracellular C termini and are considerably longer than those of the *S. cerevisiae* Ste3 pheromone receptor. Thus, specific intracellular binding sites for regulatory proteins could be present and might also perform a function in the regulation of expression. This prompted us to measure expression levels with quantitative RT-PCR in the transformant Vbar2t, which carries only the one truncated receptor gene (*bar2t*) but lacks all other *B* mating genes. The expression level of *bar2t* was determined to be slightly higher than the expression level of *bar2* in a wild-type strain at t_0 (Fig. 3D). The induction of expression upon mating was lower, however. The truncated gene also showed a slower increase in expression, which prompted us to carefully reexamine its phenotype.

C-terminal truncation of the pheromone receptor affects clamp fusion. We examined the B_{null} transformants containing either the entire, full-length pheromone receptor gene *bar2f* or the truncated version, *bar2t*, in order to investigate the potential functions of the long intracellular C terminus of the receptor. Integration of either *bar2f* or *bar2t* reconstituted the wild-type phenotype of mating competence in monokaryotic, vegetative mycelium. Pheromone receptor transformants developed mycelia (substrate and aerial) that grew in a normal fashion, but with a slightly smaller colony diameter than wild-type strains (data not shown). Pheromone receptor transformants mated with fully compatible partners (A≠B≠) and showed the expected unilateral nuclear migration and formation of apparently clamped mycelium on the side of the receptor transformant. Both versions of the receptor recognized pheromones of all other *B*α specificities but the self-specificity *B*α*2*, and clamp structures were formed at every septum. In transformants carrying a truncated receptor gene, a delay in development was seen, with these matings taking 1 to 2 days longer before clamp cells became visible, correlating well with the delayed upregulation of receptor and pheromone gene expression measured by RT-PCR. Closer examination of all fully compatible crosses (*A*≠*B*≠) involving transformants carrying either *bar2f* or *bar2t* alleles revealed the formation of pseudoclamps with a trapped nucleus in the unfused hook cells (Fig. 5). The tip cells of mated receptor transformants contained two nuclei and hence were dikaryotic. Subterminal cells often contained only one nucleus, while the other remained trapped in the unfused pseudoclamp (Fig. 5). For analysis, we classified four states of clamp fusion: (i) three successive clamps behind the tip cell are fused clamps, (ii) only the first clamp (closest to the tip cell) is still unfused, (iii) all three clamp connections are pseudoclamps, and (iv) an alternate distribution of pseudoclamps and fused clamps occurs (Fig. 6). Using this classification, it was observed that in wild-type mating interactions, clamp fusion in tip cells was not (yet) completed in 35% of the cases, while all subterminal cells had only fused clamps. In transformants carrying either *bar2f* or *bar2t*, however, all four patterns occurred, albeit with a higher rate of clamps in the transformant with the full-length gene *bar2f* (Fig. 6). Thus, the 118 aa missing from the C terminus in Vbar2t influence the correct and timely development of dikaryotic hyphae.

Truncation of Bar2 affects fruit body development and spore production. Despite the formation of pseudoclamps, the receptor transformants Vbar2f and Vbar2t were able to develop fruit bod-

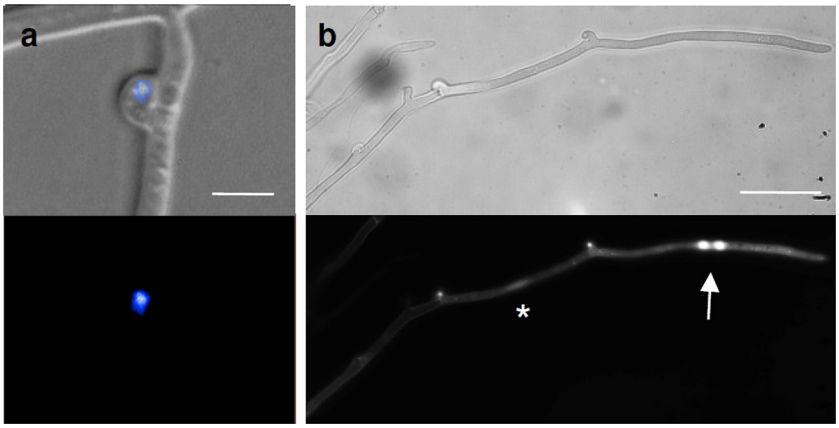

FIG 5 Pseudoclamp formation in transformants carrying the truncated pheromone receptor gene *bar2t* after a compatible mating. (a) Pseudoclamp with a DAPI-stained nucleus trapped in the unfused clamp. Bar, 5 μm. (b) Bright-field micrograph of hyphae and DAPI staining of nuclei showing a nuclear pair in the tip cell and the two nuclei separated in the unfused clamp and subterminal cell (asterisk). The tip of the hypha is at the extreme right of the figure, and nuclei are indicated by an arrow. Bar, 20 μm.

ies. However, fruit body development often stopped before maturity. Lamellae were either absent or malformed, but production of spores was recorded nevertheless (Fig. 7). The spores produced from transformants carrying *bar2t* lacked nuclei in high proportions (>70%). The majority of the spores of receptor transformant Vbar2t showed only mitochondrial DNA staining, appearing as small spots distributed all over the cell (Fig. 8). However, a small proportion of nucleated spores was formed in transformant Vbar2t, and these were able to germinate and to develop into monokaryotic mycelia. This is in contrast to the wild type, where spores generally contain two nuclei per spore (Fig. 8) and germinated at almost 100%. Transformants carrying *bar2f* showed an intermediate phenotype, with anucleated spores and wild-type-like spores being observed (Fig. 8).

Cellular localization of pheromone receptor. We decided to utilize the enhanced level of pseudoclamps for *in vivo* and *in situ* localization of receptor molecules. The prolonged presence of unfused clamp cells allowed us to examine the short-distance attraction between interacting cells. For this purpose, the receptor gene *bar2t* C-terminally fused to both Gfp and HA allowed us to perform both *in vivo* observations and immunofluorescence staining of fixed cells, respectively. When this fusion construct was transformed into the B_{null} recipient strain, complementation was observed for mating functions with all non-self-*B*α specificities, as was the case for the untagged pheromone receptors. The hyphae produced from the matings showed the expected occurrence of pseudoclamps, with no apparent effect of the Gfp-HA tag on receptor function.

Expression of the Gfp-tagged receptor was induced by a mating interaction with a compatible wild-type strain, and fluorescence could be detected in pseudoclamps, at the cell periphery, and in vesicles (Fig. 9). Thus, *in vivo* visualization confirmed the presence of receptor molecules within pseudoclamps, while staining of the nuclear envelope was never observed. To independently confirm the results, the same transformants were used for immunofluorescence detection of the receptor. At the low expression levels observed for the receptor gene, we reasoned that the signal enhancement inherent in antibody detection would be of benefit to our analyses. Localization of the receptor with predominant occurrence at the cell periphery was consistent with our observations of membrane localization in pseudoclamps and clamp connections, utilizing an FITC-labeled antibody specific for the HA tag (Fig. 9).

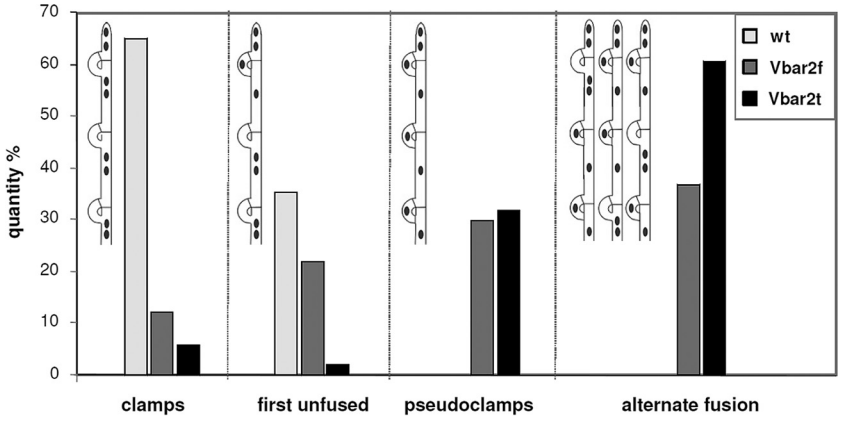

FIG 6 States of clamp fusion in a wild-type (wt) dikaryon (12-43 × 4-39) and in two pheromone receptor transformants carrying either the full-length gene *bar2f* (Vbar2f) or the truncated version, *bar2t* (Vbar2t), after interacting with a compatible mating partner (strain 4-39); $n = 100$.

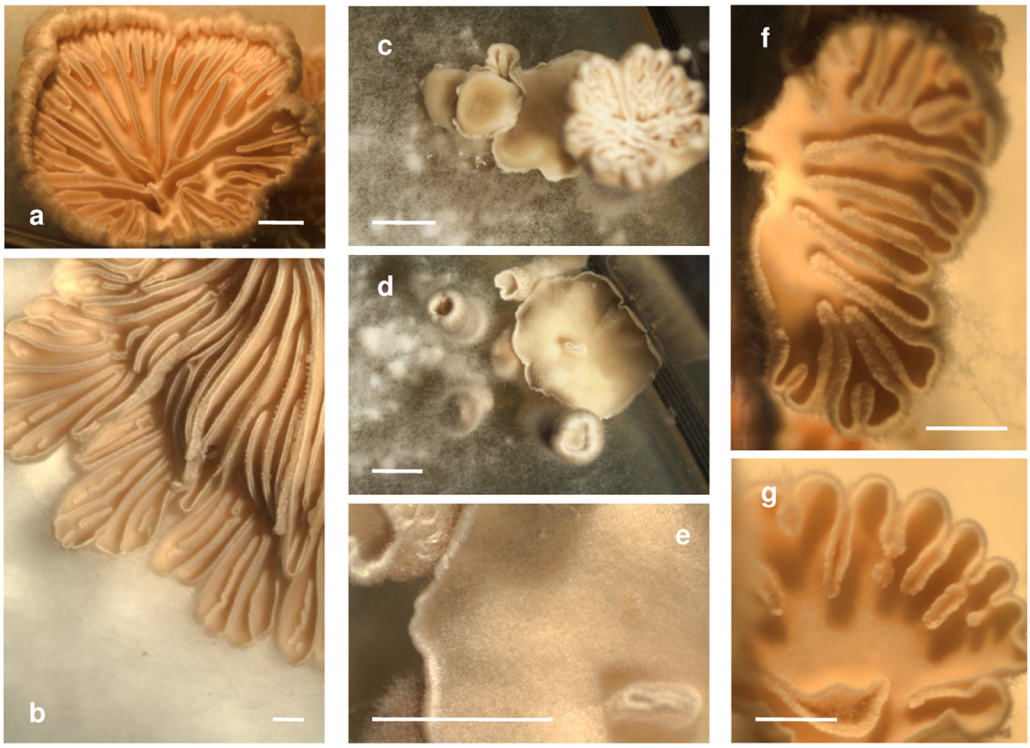

FIG 7 Fruiting bodies of *Schizophyllum commune* in the wild type (a and b), pheromone receptor transformant Vbar2t with the truncated receptor (c to e), and the pheromone receptor transformant Vbar2f with the full-length receptor gene (f and g). All strains have been mated with the compatible partner strain 4-39. While the wild type forms fruit bodies with ordinary pseudolamellae, the transformants show defects in fruit body development, resulting in fewer or absent pseudolamellae. Bars, 0.5 cm.

The fluorescence signal was especially intense at the septa, which we interpret to be a result of cell membranes on both sides of a single septum. For some pseudoclamps, detection of Gfp-tagged receptor failed, presumably for those trapping a wild-type nucleus not carrying Gfp.

Since the expression of pheromone receptor protein was shown to be induced in compatible mating interactions, fluorescence analyses were performed predominantly on mycelia derived from mated cultures. When monokaryotic, vegetative mycelium of the tagged Gfp-receptor transformants was investigated, no clear fluorescence signal was detectable for either Gfp or HA, because of the extremely low expression levels under these conditions (data not shown). Mycelia of untagged wild-type strains were used as negative controls in fluorescence microscopy.

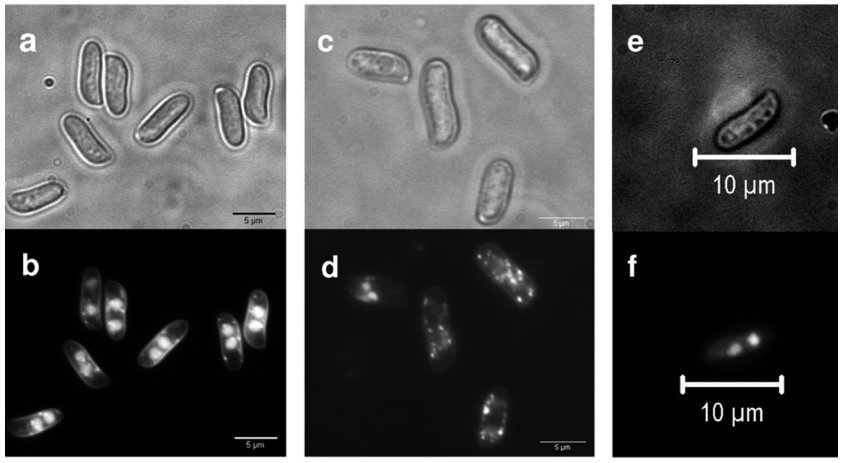

FIG 8 Spores of *Schizophyllum commune* in the wild type (a and b) or pheromone receptor transformants encoding either the truncated receptor (Vbar2t) (c and d) or the full-length receptor (Vbar2f) (e and f). Spores were obtained from fruiting bodies generated from compatible crosses with strain 4-39. While almost all wild-type spores contained two nuclei (b), more than 70% of the spores from the truncated receptor transformants did not contain nuclei and only mitochondrial DNA was stained (d). The spores derived from outcrosses of the full-length receptor transformant Vbar2f showed a higher incidence of two nuclei than spores derived from outcrosses with the truncated version (f).

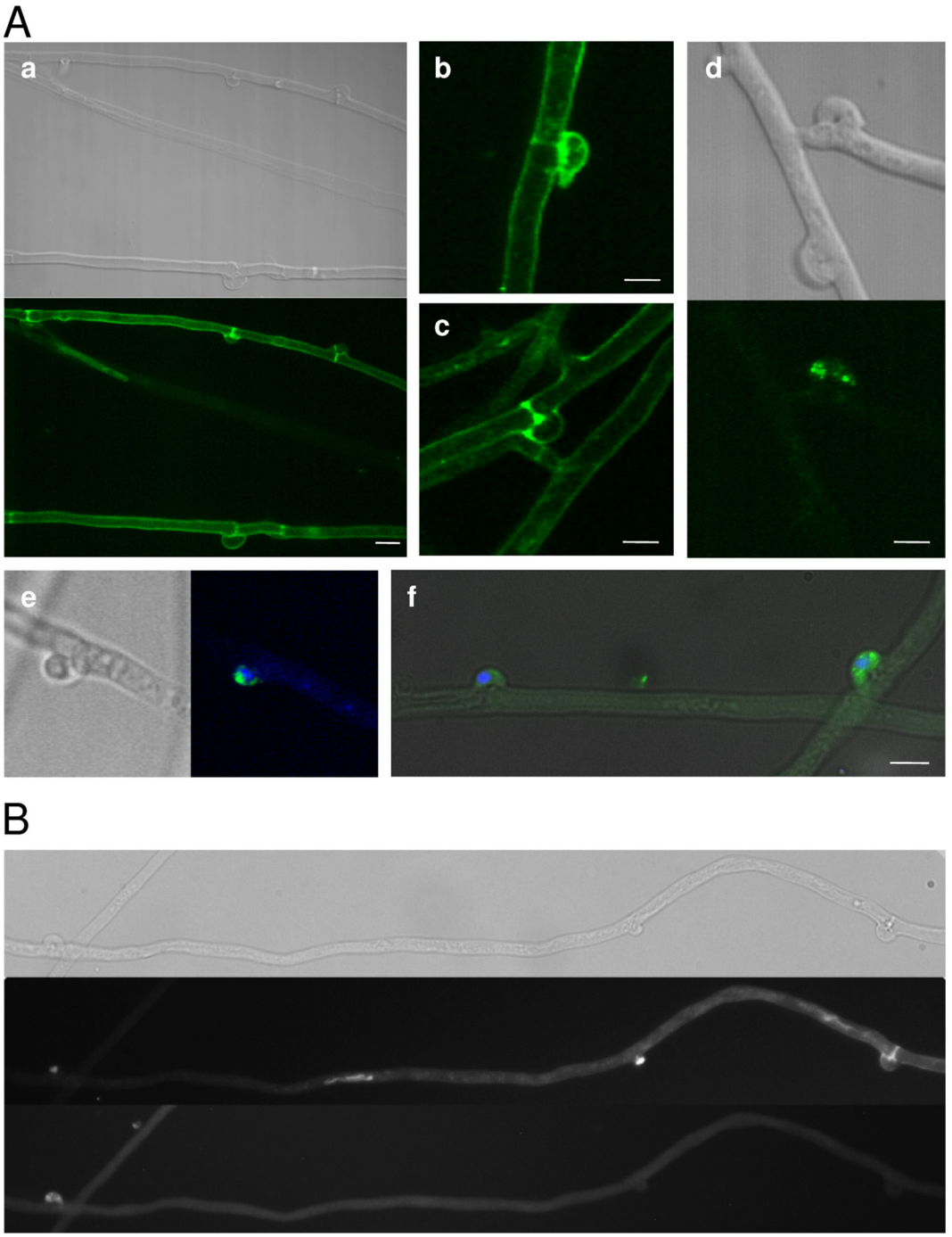

FIG 9 (A) Micrographs of HA-Gfp-tagged pheromone receptor localization in dikaryotic *S. commune* transformants by immunostaining (Aa to Ad) and *in vivo* (Ae and Af) in dikaryotic mycelium (Vbar2tG1 or Vbar2tG11 mated to 4-39); (B) differentiation of pseudoclamps showing strong receptor staining while others are nonfluorescent (top, bright field; middle, DAPI and calcofluor; bottom, Gfp). Bars, 5 μm.

Downstream signaling and target genes of pheromone response. In order to identify genes responding to pheromone signaling at the transcriptional level, we used whole-genome microarrays hybridized with cDNA derived from different mating interactions. These interactions included the heterokaryotic A_{on}, heterokaryotic B_{on}, and dikaryotic (A_{on} and B_{on}) conditions. Overall, 26% of the entire genome was determined to be transcriptionally regulated (fold change, ≥2; $P \leq 0.05$) due to mating interactions. This can be broken down into 974 genes (7% of the genome) regulated by activation of the *A* pathway, 1,480 genes (11% of the genome) regulated by the *B* pathway, and 1,016 genes (8% of the genome) regulated by both *A* and *B*. The last type of regulation was not analyzed further, since mushroom formation would likely override or obscure any direct effects of combined *A* and *B* regulation. A higher threshold for transcriptional regulation (change, ≥5-fold) yielded 89 *A*-regulated genes (41 up, 48 down;

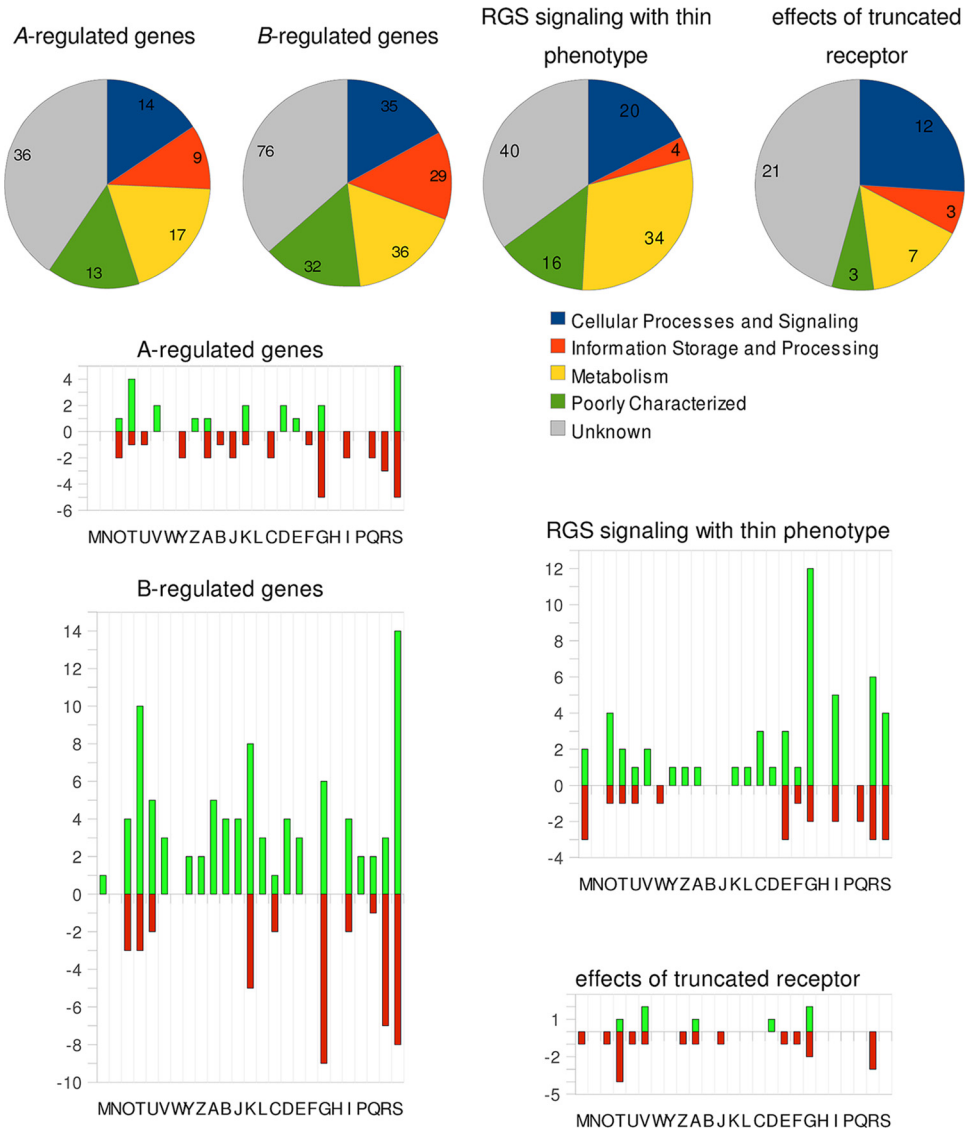

FIG 10 Transcriptional regulation of genes associated with various mating interactions in *S. commune*. Functional groups of regulated genes (change, ≥5-fold; $P \leq 0.05$; green, upregulation; red, downregulation). KOG classification: cellular processes and signaling (M, cell wall/membrane/envelope biogenesis; N, cell motility; O, posttranslational modification, protein turnover, chaperones; T, signal transduction; U, intracellular trafficking, secretion, and vesicular transport; V, defense mechanisms; W, extracellular structures; Y, nuclear structure; Z, cytoskeleton), information storage and processing (A, RNA processing and modification; B, chromatin structure and dynamics; J, translation, ribosomal structure and biogenesis; K, transcription; L, replication, recombination, and repair), metabolism (C, energy production and conversion; D, cell cycle control, cell division, chromosome partitioning; E, amino acid transport and metabolism; F, nucleotide transport and metabolism; G, carbohydrate transport and metabolism; H, coenzyme transport and metabolism; I, lipid transport and metabolism; P, inorganic ion transport and metabolism; Q, secondary metabolites biosynthesis, transport and catabolism), and poorly characterized (R, general function prediction only; S, function unknown).

see Tables S2 to S4 in the supplemental material) and 208 *B*-regulated genes (138 up, 70 down; see Tables S2, S5, and S6 in the supplemental material), corresponding to 0.7% and 1.6% of the genome, respectively. According to KOG (euKaryotic Orthologous Groups) classification, putative protein domains and general functions for the obtained regulated genes were classified (Fig. 10).

As is evident from this analysis, more genes were regulated by activation via action of the *B* mating type genes than through the *A*-dependent pathways. We found that the *A* mating type genes, which code for homeodomain transcription factors, primarily activate genes involved in signal transduction, defense mechanisms, transcription, and cell cycle control, while genes involved in carbohydrate metabolism are downregulated. Specifically, the increased expression of genes coding for a splicing coactivator subunit (protein identifier [ID] 234140) and the large subunit of an RNA polymerase II (ID 112761) hints to an enhancement of transcriptional activity (Table 2).

In contrast to the *A* pathway, the response to *B* activation was associated with more than 2-fold the number of transcriptionally regulated genes. Most of the differentially expressed genes are upregulated and involved in information storage, metabolism, and

TABLE 2 Identification of genes differentially expressed under *A*-regulated development ordered by KOG group

Regulation, KOG group[a]: (gene name) protein function/biological process/cellular component	Protein ID	Fold change in expression
Upregulated		
O: E3 ubiquitin ligase interacting with arginine methyltransferase, Zn finger, CCHC type	107850	8.3
T: (*aay4*) large RNA-binding protein (RRM superfamily), A-α-Y mating type-dependent binding region, A-α-Y4 protein; HD2	231556[b]	11.9
T: (*clp3*) Clp1-like protein, mitochondrial carrier	233611	5.9
T: G-protein beta WD-40 repeat	107647	5.8
T: cAMP-dependent protein kinase catalytic subunit (PKA)	233600	5.5
T: (*bpl1*) pheromone precursor	112470	5.5
V: heme peroxidase, plant/fungal/bacterial, response to oxidative stress	106700	11.1
V: (von Willebrand factor and related) coagulation proteins	256712	5.1
Z: dystonin, GAS (growth-arrest-specific protein), and related proteins	232734	7.7
A: splicing coactivator SRm160/300, subunit SRm300	234140	5.5
K: RNA polymerase II, large subunit	112761	5.2
D: warts/lats-like serine threonine kinases, serine/threonine protein kinase	60342	20.3
D: checkpoint kinase and related serine/threonine protein kinases, serine/threonine protein kinase	111399	9.9
E: peptidase M, neutral zinc metallopeptidases, zinc-binding site	235599	7.5
G: chitinase	110277	18.2
G: glycoside hydrolase, chitinase active site	234329[b]	5.1
S: cyclin-like F box	108012	21.0
S: Zn finger domain, MYND type	237371	11.1
S: cyclin-like F box	234092	9.3
S: Zn finger, C2H2 type, nucleic acid binding	110202	6.5
S: flank to A genes, hypothetical proteins in *Laccaria bicolor* (NCBI accession no. XP_001886997.1) and *C. cinerea* (NCBI accession no. XP_001840121.2) by BLASTp analysis	241485	6.1
O: transport protein Sec61, alpha subunit, protein secretion, P—P bond hydrolysis-driven protein transmembrane transporter activity	234899	−76.0
O: molecular chaperone (DnaJ superfamily), heat shock protein binding	49803	−5.7
T: EPS15 homology, synaptic vesicle protein EHS-1 and related EH domain proteins	113426	−14.7
U: transport protein particle (TRAPP) complex subunit, Bet3	14103	−16.0
Y: nucleolar GTPase/ATPase p130	234188	−83.9
Y: nucleolar GTPase/ATPase p130	233086	−5.5
A: helix-turn-helix, Fis type, splicing factor 1/branch point binding protein (RRM superfamily)	54550	−8.7
A: RNase, RNase III	30567	−5.1
B: predicted histone tail methylase containing SET domain	107557	−5.2
J: translation initiation factor 5B (eIF-5B), phosphotransferases with an alcohol group as acceptor	14724	−17.3
J: mitochondrial ribosomal protein L16	33729	−7.3
K: thyroid hormone receptor-associated protein complex, subunit TRAP230	47014	−9.6
C: NADH-cytochrome b_5 reductase, flavoprotein pyridine nucleotide cytochrome reductase	231100	−25.0
C: (*R*,*R*)-butanediol dehydrogenase, FAD-linked oxidase, N terminal	63691	−8.8
F: dihydroorotase and related enzymes, urease	16734	−26.7
G: cellulose-binding region, fungal, esterase, poly-β-hydroxybutyrate depolymerase, esterase/lipase/thioesterase	236921	−24.0
G: glycosyltransferase, family 8 glycogenin, glycogenin glucosyltransferase	73723	−14.6
G: dimeric dihydrodiol dehydrogenase, *trans*-1,2-dihydrobenzene-1,2-diol dehydrogenase	54187	−9.8
G: glycoside hydrolase, family 61	58521	−6.2
G: predicted transporter (major facilitator superfamily), L-arabinose isomerase	76389	−5.8
I: cytochrome P450 CYP4/CYP19/CYP26 subfamilies, unspecific monooxygenase	67567	−6.7
I: peroxisomal 3-ketoacyl coenzyme A-thiolase P-44/SCP2, thiolase	67156	−6.1
Q: zinc-containing alcohol dehydrogenase superfamily, sorbitol dehydrogenase, L-iditol 2-dehydrogenase	64180	−13.5
Q: dehydrogenases with different specificities (related to short-chain alcohol dehydrogenases), glucose/ribitol dehydrogenase	234748	−9.0
R: predicted transporter (major facilitator superfamily), similar to drug-resistant transporter EmrB/QacA	44593	−13.5
R: monodehydroascorbate/ferredoxin reductase, FAD-dependent pyridine nucleotide-disulfide oxidoreductase	82230	−10.4
R: predicted yippee-type zinc-binding protein	58559	−8.0
S: mitochondrial carrier domain	258521[c]	−126.6
S: [ribulose-bisphosphate-carboxylase]-lysine *N*-methyltransferase, nuclear protein SET	59023	−14.0
S: winged helix-turn-helix transcription repressor DNA binding	113352	−7.3
S: dimethylmenaquinone methyltransferase	57620	−5.9
S: Zn finger domain, MYND type	109469	−5.9

[a] KOG groups are defined in the legend to Fig. 10.
[b] Additionally upregulated in thin phenotype.
[c] Additionally downregulated in thin phenotype.

signal transduction via 3′-5′-cyclic AMP (cAMP) phosphodiesterase and small G proteins (for example, *S. cerevisiae* Pde1 [ID 105393]; GAP [ID 108327], and a signaling protein [ID 62504]). Fewer downregulated genes were detected, and these were mostly classified to either the metabolism of carbohydrates (IDs 31488, 55688, 13089, 70398, 108884, 13397, 110470, 109961, 236244), transcription (IDs 61956, 35685, 65707, 114395, 256713), or posttranslational modification, protein turnover, and chaperones (IDs 56996, 17256, 83759) (Table 3).

Intracellular modification of pheromone signaling. To obtain more information on cellular pathways involved in sexual development, we investigated several mutant strains affected in mating interactions. The influence of Thn1 was examined by the expression profiling of a homokaryotic *S. commune* strain expressing a thin phenotype. The 114 regulated genes (72 up, 42 down) (Fig. 10; see Tables S7 and S8 in the supplemental material) showed high overlap with cellular responses, in accordance with the known RGS function of Thn1 as a repressor of G-protein-coupled signaling. Upregulated genes included those influencing processing and posttranslational modification or genes with a stress-related protein function. Proteins involved in biogenesis of the cell wall or membrane turnover were identified among both the up- and downregulated genes, suggesting reprogramming of the cells via genetic means (Table 4; see also Tables S7 and S8 in the supplemental material). Among the upregulated genes, we also found several candidates for chitinases (IDs 85084, 85210, 46134, 79630) and other glycoside hydrolases (family 61, IDs 60863, 16233, 41145; family 5, ID 16928; others, ID 234329), suggesting functions associated with a reorganization of the cell wall. The expression of *thn1* itself was highly downregulated in a loss-of-function *thn* mutant compared to a wild-type homokaryon (Table 4).

The truncation of the intracellular C terminus of the receptor would be predicted to interfere with some intracellular protein-protein interactions upon pheromone stimulation. Only 25 genes with predicted function (46 in total) were altered in expression at least 5-fold (Fig. 10; Table 5; see also Tables S9 and S10 in the supplemental material). A strong effect on genes involved in cellular processes and signaling was observed, with changes ranging from 10- to 60-fold in magnitude. Of specific interest was the finding that a small GTPase involved in nuclear protein import (ID 43735) was downregulated more than 1,000-fold (Table 5).

DISCUSSION

The localization of the pheromone receptor protein in hyphae of the fungus *S. commune* provides an important link between pheromone perception and the cellular responses to that signal (55). In this study, the pheromone receptor was visualized at the cell periphery, consistent with a localization in the plasma membrane. No evidence of nuclear membrane localization, as has been proposed in some previous hypotheses, was found (5, 60). Another prediction of these models was that pheromone receptors would be expected to be localized in the plasma membrane close to the encoding nucleus by virtue of localized expression and incorporation. We did not observe an increased occurrence of fluorescence label in areas close to one of the nuclei in the dikaryotic cells. The involvement of pheromone activity in nuclear pairing could not be verified by receptor localization *in vivo* and *in situ*.

Prior unsuccessful attempts to localize the pheromone receptors in mushroom-forming basidiomycetes with Gfp labeling were attributed to the low level of expression of the *B* genes, also confirmed in this study. For these reasons, it seemed of vital importance to determine the critical parameters necessary for high receptor expression under natural conditions. This goal was greatly facilitated by the induction of mating in many hyphal compartments at the same time through the setup consisting of a top-to-top sandwich formed from two pregrown mycelia. This experimental system allowed us to define the period of highest expression to a time between 6 and 12 h in mating interactions of compatible strains. To the best of our knowledge, this is the first time that a pheromone receptor has been localized in the hyphae of a mushroom-forming fungus.

Because the *B* genes regulate both nuclear migration and the fusion of clamp cells, pheromone activity could be envisioned to play a key role in the upregulation of pheromone expression in as yet unfused clamps. It follows that pheromone receptors would be expected to be localized to the plasma membrane of pseudoclamps and to the hyphal cell close to the fusion site. However, localization studies were hampered by both the low expression level of the pheromone receptors and the transient nature of hook cell formation, which is normally completed along with a fused clamp connection within seconds (59). The unexpected finding that clamp cell fusion was inhibited in mated mycelium of receptor transformants carrying a C-terminally truncated receptor gene enabled us to detect a fluorescence signal predominantly in unfused pseudoclamps. The Gfp-tagged receptor could be clearly localized at the cell periphery in association with the plasma membrane. In addition, septa of the clamped mycelia gave a strong signal. Mislocalization of the tagged receptor seems unlikely because transformants of the B_{null} mutant integrating this construct exhibited the normal self- versus non-self-recognition phenotype characteristic of wild-type cells. Clamp connections were formed more slowly than wild-type mating interactions, but this was also observed in nontagged truncated and full-length receptor transformants. While the transformants did contain mostly one copy of the respective gene (but in one case the transformant contained up to five copies of the respective gene), a difference in phenotype was not connected to copy number, neither for number of pseudoclamps formed or fruit body formation nor for formation of anucleate spores.

In our receptor transformants of the B_{null} recipient strain, the distribution of nuclei in mated mycelia was disturbed, with one nucleus being trapped in the unfused clamp cell and the other being trapped in the main hyphal compartment. Thus, two monokaryotic compartments were formed, resulting from the failure to achieve the dikaryotic condition after the initiation of mitosis and clamp formation. The strong fluorescence visible in pseudoclamps is an indication for mating competence associated with higher levels of receptor within that cellular structure. A fluorescent signal would be visible only in those unfused pseudoclamps trapping a transformed, Gfp-receptor-encoding nucleus and not those trapping an untransformed nucleus. Given that we did not observe fluorescence in every unfused pseudoclamp that had trapped a nucleus, this observation supports the idea of positioning of either nucleus within the newly formed clamp. However, we did not observe a regular, alternating distribution for the nuclei going into the hook cells of *S. commune*, as has been demonstrated for *C. cinerea* (24). Rather, nuclear distribution is mixed in accordance with the possibility of nuclei randomly

TABLE 3 Identification of genes differentially expressed under *B*-regulated development ordered by KOG group

Regulation, KOG group[a]: (gene name) protein function/biological process/cellular component	Protein ID	Fold change in expression
Upregulated		
M: chitinase	231665	14.7
O: molecular chaperone (DnaJ superfamily), heat shock protein DnaJ	231463	18.1
O: AAA+-type ATPase	109412	8.6
O: nuclear AAA ATPase, peptidase S16, Lon protease	58751	8.2
O: HSP90 cochaperone CPR7/cyclophilin, peptidyl-prolyl *cis-trans* isomerase, cyclophilin type	55359	6.1
T: indoleamine 2,3-dioxygenase	33516	198.5
T: signaling protein RIC-8/synembryn (regulates neurotransmitter secretion)	62504	20.1
T: G protein beta WD-40 repeat	104106	18.6
T: GTPase activator protein, Rab GTPase activator activity	108327	13.8
T: serine/threonine protein kinase	111639	13.5
T: casein kinase (serine/threonine/tyrosine protein kinase), protein kinase	106153	13.5
T: 3′,5′-cyclic nucleotide phosphodiesterase, 3′,5′-cyclic AMP phosphodiesterase activity, similar to *S. cerevisiae* Pde1	105393	10.6
T: serine/threonine protein kinase	103735	10.5
T: armadillo/beta-catenin/plakoglobin, uridine kinase, phosphoribulokinase	71870	10.2
T: signal transduction serine/threonine kinase with PAS/PAC sensor domain, protein kinase	16935	6.2
U: translocase of outer mitochondrial membrane complex, subunit TOM37/metaxin 1	83604	13.9
U: G-protein beta WD-40 repeat, prolactin regulatory element-binding protein/protein transport protein SEC12p	49920	9.3
U: endoplasmic reticulum-Golgi vesicle-tethering protein p115	110288	7.9
U: peptide exporter, ABC superfamily	51416	7.4
U: vacuolar sorting protein VPS24, Snf7, protein transport	47850	5.8
V: predicted transporter (major facilitator superfamily), tetracycline resistance protein TetB, hydrogen antiporter activity	41682	12.2
V: Von Willebrand factor and related coagulation proteins, various SH3 domains (protein destination)	255861	11.4
V: predicted transporter (major facilitator superfamily), tetracycline resistance protein TetB, similar to Mfs1.1	233429[b]	5.2
Y: nucleolar GTPase/ATPase p130	51001	12.2
Y: nucleolar GTPase/ATPase p130	256072	6.3
Z: spindle pole body protein Sad1p, peptidase C19, ubiquitin carboxyl-terminal hydrolase 2	80616	25.6
Z: myosin class V heavy chain, myosin head, motor region	70377	11.0
A: splicing coactivator SRm160/300, subunit SRm300	232813	33.0
A: splicing coactivator SRm160/300, subunit SRm300	113731	25.4
A: polyadenylation factor I complex, subunit, Yth1 (cleavage and polyadenylation specific factor [CPSF] subunit), Zn finger	13540	15.6
A: splicing coactivator SRm160/300, subunit SRm300	256249	7.9
A: tuftelin-interacting protein TIP39, contains G-patch domain, D111/G patch (mouse protein)	36337	5.7
B: SWI-SNF chromatin remodeling complex, Snf5 subunit, SNF5/SMARCB1/INI1, chromatin remodeling	53495	18.2
B: chromatin remodeling protein, contains PHD (plant homeodomain) Zn finger	233026	14.9
B: histone acetyltransferase SAGA, TRRAP/TRA1 component, phosphatidylinositol 3 and 4 kinases	12680	14.7
B: SWI/SNF chromatin-remodeling complex protein, prion protein, aminoacyl-tRNA synthetase	106231	6.9
J: 60s acidic ribosomal protein P1, structural constituent of ribosome	233634	11.5
J: tRNA methyltransferase, N_2,N_2-dimethylguanosine tRNA methyltransferase, tRNA (guanine-N_2-)-methyltransferase	81492	10.0
J: pseudouridylate synthase, tRNA pseudouridine synthase	42694	8.9
J: translation initiation factor 2C (eIF-2C) and related proteins, argonaute and dicer protein, PAZ domain	257069	6.1
K: RNA polymerase II, large subunit, DNA-directed RNA polymerase	105543	16.8
K: RNA polymerase I, large subunit, DNA-directed RNA polymerase	255115	14.8
K: transcription regulator XNP/ATRX, DEAD box superfamily, shugoshin, N terminal	256320	13.8
K: transcription coactivator, double-stranded RNA binding	104274	11.5
K: DNA-directed RNA polymerase subunit E′, RNA polymerase Rpb7, N terminal	234509	7.6
K: transcription initiation factor IIF, small subunit (RAP30); transcription initiation factor IIF, beta subunit	78184	6.5
K: transcription factor XBP-1, basic leucine zipper (bZIP) transcription factor	236086	5.7
K: GCN5-related *N*-acetyltransferase, transferring groups other than amino acyl groups	52412	5.5
L: DNA repair protein, SNF2 family, helicase, C terminal, SNF2 related	81511	306.0
L: CDC45 (cell division cycle 45)-like protein, DNA replication initiation	50273	11.7
L: origin recognition complex, subunit 4	46745	8.2
C: mitochondrial carnitine-acylcarnitine carrier protein, adenine nucleotide translocator 1	58334	17.4
D: halotolerance protein HAL3 (contains flavoprotein domain), peptidyl-prolyl *cis-trans* isomerase activity	113841	26.5
D: halotolerance protein HAL3 (contains flavoprotein domain), phosphopantothenoylcysteine decarboxylase	15072	24.3
D: Mis12, chromosome, pericentric region	14071	15.9
D: mitotic spindle checkpoint protein BUB3, WD repeat superfamily, G-protein beta WD-40 repeat	86026	5.5
E: oxoprolinase, hydantoinase/oxoprolinase, glutathione metabolism	82383	7.3
E: serine carboxypeptidases (lysosomal cathepsin A), peptidase S10, serine carboxypeptidase	40585	5.8
E: Xaa-Pro aminopeptidase, peptidase M24	58445	5.2

(Continued on following page)

TABLE 3 (Continued)

Regulation, KOG group[a]: (gene name) protein function/biological process/cellular component	Protein ID	Fold change in expression
G: glucose-6-phosphate/phosphate and phosphoenolpyruvate/phosphate antiporter	36941	22.9
G: general substrate transporter, sugar transporter superfamily	66123	14.4
G: esterase, poly-β-hydroxybutyrate depolymerase, esterase/lipase/thioesterase, carbohydrate esterase family 1 protein	47380	12.1
G: inositol monophosphatase	47747	7.7
G: beta-1,6-*N*-acetylglucosaminyltransferase, contains WSC domain	110551[c]	7.5
G: glycoside hydrolase, family 43	232782	6.6
I: acyl coenzyme A:diacylglycerol acyltransferase (DGAT)	53861	21.1
I: *S*-adenosylmethionine-dependent methyltransferases, generic methyltransferase	14559	13.5
I: cytochrome P450 CYP4/CYP19/CYP26 subfamilies, E-class P450, group I, gamma-hexachlorocyclohexane degradation, ascorbate and aldarate metabolism	233430	11.6
I: cytochrome P450 CYP4/CYP19/CYP26 subfamilies, unspecific monooxygenase, tryptophan metabolism, fatty acid metabolism	76871	6.0
P: Ca^{2+}/H^{+} antiporter VCX1 and related proteins, sodium/calcium exchanger membrane region, calcium/proton exchanger	27729	9.4
P: Ca^{2+} transporting ATPase, potassium/sodium efflux P-type ATPase, fungal type	53464	5.4
Q: multidrug/pheromone exporter, ABC superfamily	113902	53.4
Q: multidrug/pheromone exporter, ABC superfamily	258386	5.0
R: Zn finger, C2H2 type, similar to vegetative cell wall protein gp1 precursor (hydroxyproline-rich glycoprotein 1)	113591	19.2
R: WD-40 repeat-containing protein	84316	9.0
R: Zn finger, cytochrome *c* heme-binding site, electron transport activity	233610	5.7
S: UbiA prenyltransferase, prenyltransferase activity	238827	23.8
S: chloroperoxidase, peroxidase activity, electron transport	57566	21.7
S: cyclin-like F-box domain	111277	18.4
S: cyclin-like F box, Zn finger, C2H2 type	104797	8.7
S: glutathione *S*-transferase, N terminal	111982	8.3
S: bucentaur or craniofacial development	112020	8.2
S: protein binding, BTB/POZ domain	236141	7.8
S: bacterial extracellular solute-binding protein, family 3, transporter activity	105400	7.7
S: predicted membrane protein	108226	7.7
S: Zn finger, MYND type	231200	7.1
S: target SNARE coiled-coil region	56068	6.5
S: cyclin-like F box, Zn finger, C2H2 type	234065	6.3
S: Zn finger, CCHC type	237097	6.0
S: notchless-like WD-40 repeat-containing protein, 2-acetyl-1-alkylglycerophosphocholine esterase, G-protein beta WD-40 repeat	37220	5.2
Downregulated		
O: alkyl hydroperoxide reductase/peroxiredoxin	56996	−20.1
O: E3 ubiquitin ligase interacting with arginine methyltransferase, Zn finger, CCHC type	83759	−19.5
O: peptidase M28, transferrin receptor and related proteins containing the protease-associated (PA) domain	17256	−11.3
T: serine/threonine protein kinase	108101	−8.5
T: (*brl3*) fungal pheromone STE3 6-protein-coupled receptor, mating-type alpha-factor pheromone receptor activity	258344	−5.6
T: (*bbp2*) pheromone precursor	12028	−14.2
U: nuclear pore complex, Nup98 component (sc Nup145/Nup100/Nup116), ribosomal protein L9 N-terminal like	112737	−5.9
U: clathrin adaptor complex, medium chain, adaptor complexes medium subunit family	61803	−5.2
K: fungal transcriptional regulatory protein, N-terminal, fungus-specific transcription factor, DNA binding, zinc ion binding	65707	−12.8
K: transcription factor activity, similar to Cu-dependent DNA-binding protein, copper fist DNA binding	61956	−9.4
K: fungus-specific transcription factor, DNA binding, zinc ion binding	35685	−7.3
K: peptidase M, neutral zinc metallopeptidases, zinc-binding site, selective LIM domain binding factor	114395	−6.9
K: GATA-4/5/6 transcription factors, Zn finger, GATA type	256713	−6.2
C: aldehyde dehydrogenase, tyrosine metabolism, glycolysis/gluconeogenesis	258124	−7.7
C: kynurenine 3-monooxygenase and related flavoprotein monooxygenases, salicylate 1-monooxygenase	238637	−6.5
G: gluconate transport-inducing protein	108884	−25.9
G: predicted short-chain-type dehydrogenase, glucose/ribitol dehydrogenase	236244	−20.5
G: predicted short-chain-type dehydrogenase, glucose/ribitol dehydrogenase	110470	−10.0
G: general substrate transporter, permease of the major facilitator superfamily	55688	−9.6
G: dTDP-glucose 4-6-dehydratase/UDP-glucuronic acid decarboxylase, erythromycin biosynthesis	13089	−6.8
G: permease of the major facilitator superfamily	13397	−6.0
G: glycoside hydrolase family 23 protein, candidate beta-glycosidase distantly related to *N*-acetylmuramidases	31488	−5.4
G: alpha-amylase	70398	−5.2

(Continued on following page)

TABLE 3 (Continued)

Regulation, KOG group[a]: (gene name) protein function/biological process/cellular component	Protein ID	Fold change in expression
G: predicted transporter (major facilitator superfamily), sugar:hydrogen symporter activity	109961	−5.1
I: esterase/lipase/thioesterase, hormone-sensitive lipase (HSL)	85341	−8.1
I: fatty acid desaturase, Cytochrome b_5	43089	−5.1
Q: laccase, multicopper oxidase, type 1	111478	−5.2
R: Zn finger, C2H2 type, cytochrome *c* heme-binding site, electron transport	111555	−19.5
R: transposon-encoded proteins with TyA, reverse transcriptase, integrase domains in various combinations	41205	−11.2
R: oxidoreductase, electron transport	16666	−7.5
R: transposon-encoded proteins with TyA, reverse transcriptase, integrase domains in various combinations	40072	−7.4
R: reductases with broad range of substrate specificities, oxidoreductase activity	61612	−6.5
R: *O*-methyltransferase, family 2, hydroxyindole-*O*-methyltransferase, *S*-adenosylmethionine-dependent methyltransferase (SAM) activity	238432[c]	−5.5
R: monodehydroascorbate/ferredoxin reductase, flavin adenine dinucleotide-dependent pyridine nucleotide-disulfide oxidoreductase, electron transport	62520	−5.1
S: pyridoxamine 5′-phosphate oxidase-related, flavin mononucleotide binding	42417	−17.7
S: *S*-adenosylmethionine-dependent methyltransferase, *S*-adenosylmethionine (and some other nucleotide) binding motif	80619	−9.9
S: D-alanyl–D-alanine endopeptidase activity, peptidase A22B, minor histocompatibility antigen H13, aspartic-type endopeptidase activity	58664	−8.5
S: cell growth regulatory protein CGR11	238935	−7.9
S: cyclin-like F box	110269	−7.7
S: thaumatin, pathogenesis related	111995	−6.3
S: variant SH3 domain	65138	−6.1
S: cyclin-like F box	114268	−5.7

[a] KOG groups are defined in the legend to Fig. 10.
[b] Additionally downregulated in thin phenotype.
[c] Additionally upregulated in thin phenotype.

passing each other within a hyphal compartment upon nuclear migration (11, 36, 37).

Endocytosis and replacement of receptor molecules or, alternatively, the strong expression and membrane incorporation of new receptor molecules are needed to allow the localization *in situ* and *in vivo* in pseudoclamps without diffusion of the label into adjacent cells. In our study with the truncated Gfp-labeled pheromone receptor, we could detect the receptor in vesicles and endosomes, cellular structures known to be involved in receptor internalization and degradation after induction with pheromone in *S. cerevisiae* (34). In *S. cerevisiae*, Ste3 pheromone receptor protein is short-lived and is rapidly removed from the cell surface via endocytosis (10, 57). The recycling of pheromone receptor via constitutive endocytosis has also been described for *U. maydis*, where the tagged pheromone receptor Pra1::Gfp is internalized by early endosomes and localized in vacuoles (17).

To investigate processes under the respective control of *A* and *B* mating type genes, microarray analyses were performed. Since different specificities are reflected in the sequence divergence between alleles of the mating type genes, detection of these genes was limited to the specificity of the sequenced strain H4-8 ($A_{4,6}$ $B_{3,2}$). The increased expression of homeodomain protein-encoding gene *aay4* was seen in a semicompatible mating interaction of strains differing in *A* specificity. Accompanying this interaction, we also detected a strong activation of the gene *clp3*, which encodes a protein similar to Clp1 of *C. cinerea*. The Clp1 protein promotes hook cell formation in that fungus, and a loss-of-function mutant strain exhibited a clampless phenotype (23). A similar protein in *U. maydis*, Clp1, is required for the formation of dikaryotic hyphae *in planta* and also triggers the development of clamp-like structures (58). Within the *S. commune* genome, five Clp1-like proteins were identified, but only the expression of *clp3* is regulated under all tested conditions, making this the most likely candidate for transcriptional regulation during *A*-specific development. During this process, we also detected an upregulation of both a catalytic subunit of cAMP-dependent protein kinase (PKA) and dystonin, which is a growth-arrest-specific protein. Although not expected for *S. commune*, cell cycle arrest is a specific pheromone response known to occur in both *S. cerevisiae* and *U. maydis* (33, 58). Thus, transcriptome analysis can sometimes support evolutionary conservation of pathways not obvious from phenotypic observation. However, it can be inferred that during the initial stages of mating and before ongoing nuclear migration ensues, a cell cycle arrest would occur in order to synchronize the two different nuclei involved in mating.

Transcriptional regulation associated with the *B* pathway revealed a massive reorganization of metabolism and induction of several signaling pathways, even at the stringent cutoff value of 5-fold changes in expression. The downregulated gene *brl3*, which is located next to the known pheromone receptor genes at *B*α, was shown before to be highly expressed in monokaryon and decreased in mating interactions (41). The downregulation of *brl3* in pheromone response hints to a function of this gene as a repressor under homokaryotic, nonmated conditions. From the genome, the G-protein-associated downstream pathway in sexual development and involvement of $G_{\beta\gamma}$ signaling have been predicted (55). The transcriptional induction of a predicted G_{β} subunit of a heterotrimeric G protein under B_{on} conditions hints to an activating role of this G_{β} in pheromone response.

A B_{null} strain (16) which carries a large genomic deletion and has never been observed to respond to a potential mating partner has previously been used to study the function of ectopically inte-

TABLE 4 Identification of genes differentially expressed in RGS signaling with thin phenotype ordered by KOG group

Regulation, KOG group[a]: (gene name) protein function/biological process/cellular component	Protein ID	Fold change in expression compared to: Mon1	Mon2
Upregulated			
M: chitinase, glycoside hydrolase, family 18	85210	48.5	26.2
M: chitinase, glycoside hydrolase, family 18	46134	8.9	8.5
O: glutathione *S*-transferase	61450	78.0	143.0
O: molecular chaperones GRP170/SIL1, HSP70 superfamily, heat shock protein Hsp70	78951	10.2	10.2
O: predicted E3 ubiquitin ligase, Zn finger, CCHC type	112446	7.5	7.5
O: metalloendopeptidase family, mitochondrial intermediate peptidase, mitochondrial intermediate peptidase.	13586	5.9	5.2
T: serine/threonine protein kinase, fungal transcriptional regulatory protein, N-terminal, coenzyme F420-0 gamma-glutamyl ligase activity	111022	19.3	22.8
T: (*aay4*) large RNA-binding protein (RRM superfamily), A-alpha-Y mating type-dependent binding region, A-alpha-Y4 protein; HD2	231556	6.1	7.9
U: cytosolic sorting protein GGA2/TOM1, intracellular protein transport	62583	18.4	15.3
V: inositol-1,4,5-trisphosphate 5-phosphatase	232626	27.9	44.9
V: cyclin-dependent protein kinase activity	230362	9.2	8.3
Y: nucleolar GTPase/ATPase p130	112837	9.4	8.5
Z: myosin class II heavy chain	67570	17.0	13.3
A: splicing coactivator SRm160/300, subunit SRm160 (contains PWI domain), nucleic acid-directed DNA polymerase	237177	9.5	13.1
K: transcription initiation factor TFIID, subunit BDF1 and related bromodomain proteins	78700	37.1	20.4
L: tyrosyl-DNA phosphodiesterase, phosphodiesterase I	47163	22.5	15.1
C: dihydrolipoamide acetyltransferase, biotin/lipoyl attachment	75006	15.8	15.6
C: acyl carrier protein/NADH-ubiquinone oxidoreductase, NDUFAB1/SDAP subunit, fatty acid biosynthetic process	64587	15.6	16.5
C: flavin adenine dinucleotide-linked oxidase, N terminal	104138	9.7	6.1
D: putative transcription factor HALR/MLL3, involved in embryonic development	104983	8.2	8.6
E: kynurenine hydrolase, tryptophan metabolism	232621	119.0	154.0
E: indoleamine 2,3-dioxygenase, similar to tryptophan 2,3-dioxygenase, putative	113210	74.7	109.0
E: beta-lactamase	62798	14.3	8.8
F: IMP dehydrogenase/GMP reductase, purine metabolism	14863	5.7	5.1
G: glycoside hydrolase, chitinase active site	234329	62.4	44.5
G: alpha-amylase	107514	29.3	17.3
G: polygalacturonase	233414	20.7	12.6
G: glycoside hydrolase, family 61 (endoglucanase)	41145	13.9	8.4
G: cellulose-binding region, fungal, esterase, poly-β-hydroxybutyrate depolymerase, esterase/lipase/thioesterase	236921	10.2	8.0
G: chitinase, glycoside hydrolase, family 18	79630	10.0	5.9
G: glycoside hydrolase, family 5 (mannan)	16928	9.6	5.2
G: beta-1,6-*N*-acetylglucosaminyltransferase, contains WSC domain	110551	9.2	9.2
G: glycoside hydrolase, family 61	60836	8.7	15.8
G: ricin B lectin	29538	8.6	5.4
G: glycoside hydrolase, family 61 (lignocellulose)	16233	7.0	5.3
G: predicted transporter (major facilitator superfamily), sugar transporter family	56704	6.1	5.9
I: acyl coenzyme A synthetase, flavonoids, stilbene and lignin biosynthesis	49211	16.1	12.8
I: *S*-adenosylmethionine-dependent methyltransferases, generic methyltransferase	14559	12.1	8.2
I: very-long-chain acyl coenzyme A dehydrogenase, acyl coenzyme A dehydrogenase, C terminal	233523	12.0	14.7
I: fatty acid desaturase, cytochrome b_5	78094	5.7	6.7
I: predicted lipase	61780	5.1	6.6
R: synaptic vesicle transporter SVOP and related transporters (major facilitator superfamily)	237837	30.2	50.5
R: predicted dehydrogenase, steroid dehydrogenase activity, acting on the CH-OH group of donors, NAD or NADP as acceptor	84264	28.6	19.9
R: glucose dehydrogenase/choline dehydrogenase/mandelonitrile lyase (GMC oxidoreductase family)	256423	20.0	14.1
R: Zn finger, C2H2 type	113495	9.9	15.2
R: PPR repeat (pentatricopeptide, RNA binding, eventually regulation in mitochondria)	230806	9.1	5.0
R: *O*-methyltransferase, family 2, hydroxyindole-*O*-methyltransferase, *S*-adenosylmethionine-dependent methyltransferase (SAM) activity	238432	8.7	5.3
S: cyclin-like F box	54225	14.9	19.2
S: Zn finger, CCHC type	104352	8.4	9.3
S: rare lipoprotein A	38806	7.7	9.0
S: flank to A genes, hypothetical proteins in *Laccaria bicolor* (NCBI accession no. XP_001886997.1) and *C. cinerea* (NCBI accession no. XP_001840121.2) by BLASTp analysis	241485	5.9	6.7

(Continued on following page)

TABLE 4 (Continued)

Regulation, KOG group[a]: (gene name) protein function/biological process/cellular component	Protein ID	Fold change in expression compared to: Mon1	Mon2
Downregulated			
M: (*sc4*) fungal hydrophobin SC4	73533	−151.9	−156.7
M: chitinase	85084	−29.9	−20.9
M: (*sc1*) fungal hydrophobin SC1	49129	−11.0	−12.8
O: Zn finger, MYND type, ubiquitin carboxyl-terminal hydrolase	17275	−8.2	−5.8
T: (*thn1*) regulator of G protein, Thn1	83983	−92.9	−71.9
U: vacuolar sorting protein VPS1, dynamin, and related proteins, GTPase activity	61420	−9.8	−6.0
W: collagens (type IV and type XIII) and related proteins	84580	−9.6	−5.1
J: ribosomal protein L15 (large subunit)	85903	−8.6	−15.7
E: D-aspartate oxidase	55341	−29.1	−26.0
E: methionine synthase, vitamin-B_{12} independent	57220	−6.9	−9.7
F: thymidylate kinase/adenylate kinase	233884	−14.4	−8.4
G: beta-1,6-*N*-acetylglucosaminyltransferase	233751	−31.1	−16.7
G: beta-1,6-*N*-acetylglucosaminyltransferase, contains WSC domain	103498	−7.2	−11.6
I: esterase/lipase/thioesterase, hormone-sensitive lipase HSL	85341	−9.6	−8.6
I: esterase/lipase/thioesterase	69185	−7.2	−5.1
Q: dehydrogenase activity, related to short-chain alcohol dehydrogenases	234748	−7.1	−9.4
Q: cytochrome P450 CYP2 subfamily, unspecific monooxygenase, tryptophan metabolism	111260	−7.0	−7.9
R: predicted transporter (major facilitator superfamily), tetracycline resistance protein TetB, similar to Mfs1.1	233429	−82.1	−87.4
R: predicted hydrolases or acyltransferases, esterase/lipase/thioesterase	67288	−11.9	−6.7
R: Zn finger, C2H2 type, predicted hydrolase (HIT domain-containing family)	27513	−5.4	−8.3
S: mitochondrial carrier domain	258521	−9.6	−5.9
S: Zn finger, C-X8-C-X5-C-X3-H type, nucleic acid binding	63596	−9.3	−6.7
S: GCN5-related *N*-acetyltransferase	80737	−8.9	−5.3

[a] KOG groups are defined in the legend to Fig. 10.

grated receptor genes expressed under the control of their native promoters (approximately 300 bp). In these transformants, receptor expression was lower and delayed compared to wild type. This is consistent with the delay in mating response of these receptor transformants to a compatible tester strain. On the other hand, the comparatively lower expression levels might also be the consequence of the fact that no pheromone is produced by these B_{null} receptor transformants to trigger nuclear migration in the wild-type mating partner. This results in a unilateral mating (30) where only half the cells in the sandwich overlay are in fact activated for *B*-regulated development. The formation of pseudoclamps is a phenomenon which has been observed earlier in semicompatible mating interactions ($A \neq B=$), where nuclei enter the hyphae of the mating partner only at the fusion point. This results in the formation of some pseudoclamps and the death of hyphae in the fusion area (53). In contrast to these bona fide semicompatible mating interactions, the formation of pseudoclamps in mated *bar2f* and *bar2t* receptor transformants occurs throughout the colony, with higher occurrence in the latter. This phenotype remained stable, and the mated mycelium was able to develop fruiting bodies and produced spores in both types of receptor transformant matings. Nevertheless, more basidiospores arising from those matings involving transformants integrating the truncated receptor were observed to be anucleate. Thus, a role of the C terminus in nuclear migration toward the spore can also be postulated.

The intracellular regions of *S. commune* pheromone receptors are considerably longer than those found in other fungi (3, 35, 69). No influence of C-terminal truncation of *S. commune* receptors on ligand binding and pheromone discrimination like that found for C-terminal truncations of the Ste2 pheromone receptor of *S. cerevisiae* (56) has been observed (19, 20, 22). In our study, we found that the truncated *bar2t* receptor of 518 amino acids still induces *B*-regulated development, as does the 636-amino-acid full-length *bar2f* receptor. However, the downstream signal cascade seems to be affected by the truncation, the result of which is a change in the expression of downstream genes. An example of this is the small GTPase regulator (RanGEF) commonly involved in nuclear protein import, whose expression is drastically reduced in the truncated receptor transformants.

The pheromone receptors in *S. commune* are expected to interact with the RGS protein Thn1, a homolog to the *S. cerevisiae* protein Sst2. Deletion of Sst2 (Δ*sst2*) results in hypersensitivity to pheromone (2, 28, 34, 56). The deletion of *thn1* in *S. commune* also resulted in an increase of pheromone sensitivity (13). In wild-type cells, Thn1 is expected to bind to the unphosphorylated receptor protein and inhibit pheromone response prior to mating, while after ligand binding, internalization is enabled and/or turnover is increased.

We determined that the expression of *thn1* is strongly downregulated within the mutant with the *thn* mutation, which affects both *A*- and *B*-regulated signaling. An influence on the redox status, possibly related to the characteristic odor of the *thn* mutant strains by release of reduced molecules, is reflected by an upregulation of glutathione *S*-transferase and downregulation of cytochrome monooxygenase P450. The results of the present study confirm earlier observations that link cell integrity as well as cell

TABLE 5 Identification of genes differentially expressed with truncated receptor ordered by KOG group

Regulation, KOG group[a]: (gene name) protein function/ biological process/cellular component	Protein ID	Fold change in expression compared to:	
		Dik	Vbar2f
Upregulated			
T: protein-tyrosine-phosphatase	105372	8.8	8.4
V: inositol-1,4,5-trisphosphate 5-phosphatase	232626[b]	28.7	14.8
V: stress responsive protein	112004	9.2	14.7
A: splicing factor 3a, subunit 3	83890	14.7	7.7
D: protein with predicted involvement in meiosis (GSG1)	103874	5.6	7.8
G: monocarboxylate transporter	53388	6.3	9.2
G: glycoside hydrolase, family 10	15936	5.5	7.4
Downregulated			
M: (*sc1*) fungal hydrophobin SC1	49129	−23.9	−14.4
O: ubiquitin carboxyl-terminal hydrolase	113792	−45.0	−42.5
T: GTP-binding protein CRFG/NOG1 (ODN superfamily)	69329	−58.8	−37.4
T: serine-threonine phosphatase 2B, catalytic subunit	70929	−34.4	−25.8
T: ankyrin repeat protein	112035	−11.6	−7.2
T: regulator of chromosome condensation, ankyrin and BTB/POZ domains	256996	−5.4	−7.2
U: predicted small GTPase involved in nuclear protein import	43735	−1196.1	−719.6
V: heme peroxidase, response to oxidative stress	112999	−18.1	−9.5
Z: beta-tubulin	237626	−7.8	−5.7
A: peptidase, splicing coactivator SRm160/300, subunit SRm300	102823	−9.6	−10.1
J: ribosomal protein L15 (large subunit)	85903	−6.6	−7.9
E: peptidase S33, prolyl aminopeptidase; esterase/lipase/thioesterase	231359	−6.2	−5.2
F: atrazine chlorohydrolase/guanine deaminase	81437	−18.3	−10.8
G: glycoside hydrolase, family 43	109664	−14.9	−28.9
G: beta-1,6-*N*-acetylglucosaminyltransferase, glycoside hydrolase, family 71	53341	−11.8	−9.4
R: predicted 3′-5′ exonuclease	103723	−60.0	−30.9
R: FOG, Zn finger, nucleic acid binding	109000	−20.3	−11.5
R: cyclin	236990	−11.2	−6.0

[a] KOG groups are defined in the legend to Fig. 10.
[b] Additionally upregulated in thin phenotype.

wall and membrane synthesis to *B*-regulated development (47). The strong reduction of aerial mycelium formation seen in B_{on} as well as in *thn* mutants correlated, in both cases, with the absence of hydrophobin expression, as evidenced by the results of our microarray experiments.

With our study, we could localize the pheromone receptor to the cell periphery, with higher expression in unfused pseudoclamps. *B* pathway activation and its function in clamp fusion could be linked to the intracellular C terminus, where RGS binding impacts development of sexual structures and the formation of clamp connections as well as nucleated spores. Using mushroom-forming *S. commune*, pheromone signaling in a tetrapolar mating system was linked to cell biology which previously had not been apparent from investigation of other fungal systems, including the yeast *S. cerevisiae*. The transcriptome analysis could show an extensive set of genes being regulated. The phenotype reflects this fact, with extended growth of mycelia after semicompatible induction of the *B* pheromone response pathway. The study on genes regulated by mating interactions allowed us to identify processes and genes, including *clp3*, involved in regulation of mating type-dependent pathways.

ACKNOWLEDGMENTS

Alexander Gehrke and Susanne Nolden are thanked for their help. We thank J. Stephen Horton for his help with editing.

We thank ILRS and JSMC for financial support.

REFERENCES

1. **Attwood TK, Findlay JBC.** 1994. Fingerprinting G-protein-coupled receptors. Protein Eng. **7**:195–203.
2. **Ballon DR, et al.** 2006. DEP-domain-mediated regulation of GPCR signaling responses. Cell **126**:1079–1093.
3. **Bölker M, Urban M, Kahmann R.** 1992. The *A* mating type locus of *U. maydis* specifies cell signaling components. Cell **68**:441–450.
4. **Casselton LA, Olesnicky NS.** 1998. Molecular genetics of mating recognition in basidiomycete fungi. Microbiol. Mol. Biol. Rev. **62**:55–70.
5. **Debuchy R.** 1999. Internuclear recognition: a possible connection between euascomycetes and homobasidiomycetes. Fungal Genet. Biol. **27**: 218–223.
6. **De Vries L, Zheng B, Fischer T, Elenko E, Farquhar MG.** 2000. The regulator of G protein signaling family. Annu. Rev. Pharmacol. Toxicol. **40**:235–271.
7. **Dohlman HG, Apaniesk D, Chen Y, Song J, Nusskern D.** 1995. Inhibition of G-protein signaling by dominant gain-of-function mutations in Sst2p, a pheromone desensitization factor in *Saccharomyces cerevisiae*. Mol. Biol. Cell **15**:3635–3643.
8. **Dohlman HG, Song J, Ma D, Courchesne WE, Thorner J.** 1996. Sst2, a negative regulator of pheromone signaling in the yeast *Saccharomyces cerevisiae*: expression, localization, and genetic interaction and physical association with Gpa1 (the G-protein alpha subunit). Mol. Cell. Biol. **16**: 5194–5209.
9. **Edgar R, Barrett T.** 2006. NCBI GEO standards and services for microarray data. Nat. Biotechnol. **24**:1471–1472.
10. **Feng Y, Davis NG.** 2000. Feedback phosphorylation of the yeast **a**-factor receptor requires activation of the downstream signaling pathway from G protein through mitogen-activated protein kinase. Mol. Cell. Biol. **20**: 563–574.

11. **Fischer R.** 1999. Nuclear movement in filamentous fungi. FEMS Microbiol. Rev. **23**:39–68.
12. **Fowler TJ, DeSimone SM, Mitton MF, Kurjan J, Raper CA.** 1999. Multiple sex pheromones and receptors of a mushroom-producing fungus elicit mating in yeast. Mol. Biol. Cell **10**:2559–2572.
13. **Fowler TJ, Mitton MF.** 2000. *Scooter*, a new active transposon in *Schizophyllum commune*, has disrupted two genes regulating signal transduction. Genetics **156**:1585–1594.
14. **Fowler TJ, Mitton MF, Raper CA.** 1998. Gene mutations affecting specificity of pheromone/receptor mating interactions in *Schizophyllum commune*, p 130–134. *In* Griensven LJLDV, Nimegen JV (ed), Proceedings of the Fourth Meeting on the Genetics and Cellular Biology of Basidiomycetes. Mushroom Experiment Station, Horst, The Netherlands.
15. **Fowler TJ, Mitton MF, Rees EI, Raper CA.** 2004. Crossing the boundary between the *B* α and *B* β mating type loci in *Schizophyllum commune.* Fungal Genet. Biol. **41**:89–101.
16. **Fowler TJ, Mitton MF, Vaillancourt LJ, Raper CA.** 2001. Changes in mate recognition through alterations of pheromones and receptors in the multisexual mushroom fungus *Schizophyllum commune.* Genetics **158**: 1491–1503.
17. **Fuchs U, Hause G, Schuchardt I, Steinberg G.** 2006. Endocytosis is essential for pathogenic development in the corn smut fungus *Ustilago maydis.* Plant Cell **18**:2066–2081.
18. **Gentleman R, Carey V, Huber W, Irizarry R, Dudoit S.** 2005. Bioinformatics and computational biology solutions using R and Bioconductor. *In* Statistics for biology and health, 1st ed. Springer, New York, NY.
19. **Gola S, Hegner J, Kothe E.** 2000. Chimeric pheromone receptors in the basidiomycete *Schizophyllum commune.* Fungal Genet. Biol. **30**:191–196.
20. **Gola S, Kothe E.** 2003. The little difference: *in vivo* analysis of pheromone discrimination in *Schizophyllum commune.* Curr. Genet. **42**:276–283.
21. **Gorfer M, et al.** 2001. Characterization of small GTPases Cdc42 and Rac and the relationship between Cdc42 and actin cytoskeleton in vegetative and ectomycorrhizal hyphae of *Suillus bovinus.* Mol. Plant Microbe Interact. **14**:135–144.
22. **Hegner J, Siebert-Bartholmei C, Kothe E.** 1999. Ligand recognition in multiallelic pheromone receptors from the basidiomycete *Schizophyllum commune* studied in yeast. Fungal Genet. Biol. **26**:190–197.
23. **Inada K, Morimoto Y, Arima T, Murata Y, Kamada T.** 2001. The *clp1* gene of the mushroom *Coprinus cinereus* is essential for *A*-regulated sexual development. Genetics **157**:133–140.
24. **Iwasa M, Tanabe S, Kamada T.** 1998. The two nuclei in the dikaryon of the homobasidiomycete *Coprinus cinereus* change position after each conjugate division. Fungal Genet. Biol. **23**:110–116.
25. **Kniep H.** 1920. Über morphologische und physiologische Geschlechtsdifferenzierung: Untersuchungen an Basidiomyzeten. Verh. Phys.-Med. Gesell. **40**:1–18.
26. **Koltin Y, Flexer AS.** 1969. Alteration of nuclear distribution in *B*-mutant strains of *Schizophyllum commune.* J. Cell Sci. **4**:739–749.
27. **Koltin Y, Raper JR, Simchen G.** 1967. Genetic structure of incompatibility factors of *Schizophyllum commune*—the *B*-factor. Proc. Natl. Acad. Sci. U. S. A. **57**:55–62.
28. **Konopka JB, Jenness DD, Hartwell LH.** 1988. The C-terminus of the *S. cerevisiae* α pheromone receptor mediates an adaptive response to pheromone. Cell **54**:609–620.
29. **Kothe E.** 1996. Tetrapolar fungal mating types: sexes by the thousands. FEMS Microbiol. Rev. **18**:65–87.
30. **Kothe E.** 2001. Mating-type genes for basidiomycete strain improvement in mushroom farming. Appl. Microbiol. Biotechnol. **56**:602–612.
31. **Kothe E.** 2008. Sexual attraction: on the role of fungal pheromone/receptor systems (a review). Acta Microbiol. Immunol. Hung. **55**:125–143.
32. **Kronstad JW, Staben C.** 1997. Mating type in filamentous fungi. Annu. Rev. Genet. **31**:245–276.
33. **Kurjan J.** 1993. The pheromone response pathway in *Saccharomyces cerevisiae*. Annu. Rev. Genet. **27**:147–179.
34. **Moore TI, Chou CS, Nie Q, Jeon NL, Yi TM.** 2008. Robust spatial sensing of mating pheromone gradients by yeast cells. PLoS One **3**:e3865.
35. **Nakayama N, Miyajima A, Arai K.** 1985. Nucleotide sequences of *STE2* and *STE3* cell type specific sterile genes from *Saccharomyces cerevisiae.* EMBO J. **4**:2643–2648.
36. **Niederpruem DJ.** 1980. Direct studies of dikaryotization in *Schizophyllum commune.* 1. Live inter-cellular nuclear migration patterns. Arch. Microbiol. **128**:162–171.
37. **Niederpruem DJ.** 1980. Direct studies of dikaryotization in *Schizophyllum commune.* 2. Behavior and fate of multikaryotic hyphae. Arch. Microbiol. **128**:172–178.
38. **Niederpruem DJ.** 1969. Direct studies of nuclear movements in *Schizophyllum commune.* Arch. Mikrobiol. **64**:387–395.
39. **Niederpruem DJ, Jersild RA, Lane PL.** 1971. Direct microscopic studies of clamp connection formation in growing hyphae of *Schizophyllum commune*. I. The dikaryon. Arch. Microbiol. **78**:268–280.
40. **Niederpruem DJ, Wessels JGH.** 1969. Cytodifferentiation and morphogenesis in *Schizophyllum commune.* Bacteriol. Rev. **33**:505–535.
41. **Ohm RA, et al.** 2010. Genome sequence of the model mushroom *Schizophyllum commune.* Nat. Biotechnol. **28**:957–963.
42. **Palmer GE, Horton JS.** 2006. Mushrooms by magic: making connections between signal transduction and fruiting body development in the basidiomycete fungus *Schizophyllum commune.* FEMS Microbiol. Lett. **262**:1–8.
43. **Papazian HP.** 1950. Physiology of the incompatibility factors in *Schizophyllum commune.* Bot. Gaz. **112**:143–163.
44. **Parag Y.** 1962. Mutations in the *B* incompatibility factor of *Schizophyllum commune.* Genetics **48**:743–750.
45. **Pfaffl MW.** 2004. Real-time RT-PCR: Neue Ansätze zur exakten mRNA Quantifizierung. BIOspektrum **1**:92–95.
46. **Raper CA, Raper JR.** 1966. Mutations modifying sexual morphogenesis in *Schizophyllum.* Genetics **54**:1151–1168.
47. **Raper J.** 1966. Sexuality of higher fungi. The Roland Press, New York, NY.
48. **Raper JR, Antonio JPS.** 1954. Heterokaryotic mutagenesis in hymenomycetes. 1. Heterokaryosis in *Schizophyllum commune.* Am. J. Bot. **41**:69–86.
49. **Raper JR, Baxter MG, Ellingboe AH.** 1960. The genetic structure of the incompatibility factors of *Schizophyllum commune*—the *A*-factor. Proc. Natl. Acad. Sci. U. S. A. **46**:833–842.
50. **Raper JR, Hoffman RM.** 1974. *Schizophyllum commune*, p 597–626. *In* King RC (ed), Handbook of genetics. Plenum Press, New York, NY.
51. **Raper JR, Krongelb GS, Baxter MG.** 1958. The number and distribution of incompatibility factors in *Schizophyllum.* Am. Nat. **92**:221–232.
52. **Raper JR, Raper CA.** 1973. Incompatibility factors—regulatory genes for sexual morphogenesis in higher fungi. Brookhaven Symp. Biol. **25**:19–39.
53. **Raper JR, Raudaskoski M.** 1968. Secondary mutations at *B*β incompatibility locus of *Schizophyllum.* Heredity **23**:109–117.
54. **Raudaskoski M.** 1998. The relationship between *B*-mating type genes and nuclear migration in *Schizophyllum commune.* Fungal Genet. Biol. **24**: 207–227.
55. **Raudaskoski M, Kothe E.** 2010. Basidiomycete mating type genes and pheromone signaling. Eukaryot. Cell **9**:847–859.
56. **Reneke JE, Blumer KJ, Courchesne WE, Thorner J.** 1988. The carboxy-terminal segment of the yeast α-factor receptor is a regulatory domain. Cell **55**:221–234.
57. **Roth AF, Sullivan DM, Davis NG.** 1998. A large PEST-like sequence directs the ubiquitination, endocytosis, and vacuolar degradation of the yeast **a**-factor receptor. J. Cell Biol. **142**:949–961.
58. **Scherer M, Heimel K, Starke V, Kamper J.** 2006. The Clp1 protein is required for clamp formation and pathogenic development of *Ustilago maydis.* Plant Cell **18**:2388–2401.
59. **Schubert D, Raudaskoski M, Knabe N, Kothe E.** 2006. Ras GTPase-activating protein Gap1 of the homobasidiomycete *Schizophyllum commune* regulates hyphal growth orientation and sexual development. Eukaryot. Cell **5**:683–695.
60. **Schuurs TA, Dalstra HJ, Scheer JM, Wessels JG.** 1998. Positioning of nuclei in the secondary mycelium of *Schizophyllum commune* in relation to differential gene expression. Fungal Genet. Biol. **23**:150–161.
61. **Schwalb MN, Miles PG.** 1967. Morphogenesis of *Schizophyllum commune.* I. Morphological variation and mating behavior of the *thin* mutation. Am. J. Bot. **54**:440–446.
62. **Schwalb MN, Miles PG.** 1967. Morphogenesis of *Schizophyllum commune.* II. Effect of microaerobic growth. Mycologia **59**:610–622.
63. **Specht CA.** 1995. Isolation of the *B*α and *B*β mating type loci of *Schizophyllum commune.* Curr. Genet. **28**:374–379.
64. **Spellig T, Bölker M, Lottspeich F, Frank RW, Kahmann R.** 1994. Pheromones trigger filamentous growth in *Ustilago maydis.* EMBO J. **13**: 1620–1627.
65. **Stamberg J, Koltin Y.** 1974. Recombinational analysis of mutations at an incompatibility locus of *Schizophyllum.* Mol. Gen. Genet. **135**:45–50.
66. **Stankis MM, et al.** 1992. The *A*α mating locus of *Schizophyllum commune* encodes two dissimilar multiallelic homeodomain proteins. Proc. Natl. Acad. Sci. U. S. A. **89**:7169–7173.

67. **Vaillancourt LJ, Raudaskoski M, Specht CA, Raper CA.** 1997. Multiple genes encoding pheromones and a pheromone receptor define the *B*β 1 mating type specificity in *Schizophyllum commune*. Genetics **146**:541–551.
68. **Vandesompele J, et al.** 2002. Accurate normalization of real-time quantitative RT-PCR data by geometric averaging of multiple internal control genes. Genome Biol. **3**:1–11.
69. **Wendland J, Kothe E.** 1996. Allelic divergence at *B*α 1 pheromone receptor genes of *Schizophyllum commune*. FEMS Microbiol. Lett. **145**:451–455.
70. **Xue C, Hsueh YP, Heitman J.** 2008. Magnificent seven: roles of G protein-coupled receptors in extracellular sensing in fungi. FEMS Microbiol. Rev. **32**:1010–1032.